

Particle Affinity for Oil-Water Interfaces and Selective Adsorption

A Dissertation
Presented to
The Academic Faculty

by

Scott D. Essenmacher

In Partial Fulfillment
of the Requirements for the Degree
Master of Science in the
School of Chemical & Biomolecular Engineering

Georgia Institute of Technology
August 2018

Copyright © 2018 by Scott D. Essenmacher

Particle Affinity for Oil-Water Interfaces and Selective Adsorption

Approved by:

Dr. Sven H. Behrens, Co-Advisor
School of Chemical & Biomolecular Engineering
Georgia Institute of Technology

Dr. J. Carson Meredith, Co-Adviser
School of Chemical & Biomolecular Engineering
Georgia Institute of Technology

Dr. Blair Brettmann
School of Materials Science and Engineering
Georgia Institute of Technology

Date Approved: May 1, 2018

ACKNOWLEDGEMENTS

I would like to thank my advisors, Dr. Sven Behrens and Dr. Carson Meredith, for their guidance and support during my graduate career. They have given some sound advice that I hope to use to my benefit in the future phases of my professional career.

I would also like to thank Dr. Blair Brettmann for being part of my committee and providing valuable feedback on my work.

I have been fortunate to be a part of two excellent research groups in the Behrens and Meredith labs. For that, I must thank those group members for the great discussions and help they provided when necessary.

Finally, I would like to thank my family and friends for their support and encouragement.

TABLE OF CONTENTS

ACKNOWLEDGEMENTS	iii
LIST OF TABLES	vi
LIST OF FIGURES	vii
LIST OF SYMBOLS	x
LIST OF ABBREVIATIONS	xi
SUMMARY	xii
CHAPTER 1: Introduction	1
1.1 Flotation Process Improvements	1
1.1.1 Particle Surface Modifications with Promoters	1
1.1.2 Oil-Coated Air Bubbles for Particle Separation	2
1.2 Objective	3
CHAPTER 2: Oil-Particle Interactions and Foam Formation	3
2.1 Overview	4
2.2 Background and Theory	5
2.3 Oil and Particle Selection	9
2.4 Methods	13
2.4.1 Foam Production	14
2.4.2 Foam Properties	14
2.4.3 Confocal Microscopy	16
2.5 Results	17
2.5.1 Foaming Ability	17
2.5.2 Foam Stability	21
2.5.3 Confocal Microscopy	25
2.6 Concluding Remarks	29
CHAPTER 3: Strength of Particle Affinity for Oil-Water Interface	32
3.1 Overview	32
3.2 Background and Theory	32
3.3 Methods	34
3.3.1 Pendant Drop Tensiometry	34
3.3.2 Three Phase Contact Angle	35
3.3.3 Particle Size	37

3.4	Results	39
3.4.1	Pendant Drop Tensiometry	39
3.4.2	Three Phase Contact Angle	41
3.4.3	Average Particle Sizes	43
3.4.4	Particle Affinity for Oil-Water Interface	45
3.5	Concluding Remarks	46
CHAPTER 4: Conclusions and Recommendations		49
APPENDIX A: Miscellaneous Figures		52
REFERENCES		54

LIST OF TABLES

Table 1. Experimental and literature oil-water interfacial tension values along with the temperature.	40
Table 2. Numerical values of the contact angles displayed in Figure 30.	42
Table 3. Average particle sizes.	45

LIST OF FIGURES

- Figure 1.** Diagram showing the requirements for successful oil and particle combinations. 4
- Figure 2.** Example showing the location of the three phase contact angle and the directions of the interfacial tensions of each interface. 5
- Figure 3.** Left: Proposed structure of capillary foams (i). The system contains a continuous liquid phase (Water), a vapor phase (Air), a secondary fluid phase (Oil), and a solid phase (Particles). The solid particles should have a high affinity to the Water/Oil interface. Choosing the right composition of the four components and agitating the mixture yields a space-spanning network of particles in water (ii) connected by bridges of oil (iii), with bubbles of air embedded in the network (iv) via a stabilizing hybrid coating of oil and particles (v), adapted with permission from Zhang et al²⁸. Copyright 2014 American Chemical Society. Right: Scanning electron microscopy images of oil-bridged particles (a) and bubble coating in a capillary foam (b), taken with permission from Zhang et al²⁴. 8
- Figure 4.** The preferred emulsion types based on Winsor's R ratio. The preferred emulsion when $R = 1$ is a bicontinuous structure microemulsion. 11
- Figure 5.** All the oils (left column) and particles (right column) used. 12
- Figure 6.** Diagram of the procedure used to create foams 14
- Figure 7.** Example of how froth height is determined. 15
- Figure 8.** Averages of at least three measured froth heights of foams created with 10 wt% PVC and 1 wt% oil. The control does not contain oil. 17
- Figure 9.** Typical foams with 10 wt% PVC and 1 wt% oil within 1 hour after production. The control does not contain oil. 17
- Figure 10.** Averages of at least three measured froth heights of foams created with 5 wt% PS and 1 wt% oil. The control does not contain oil. The blue bar is the average froth height for foams created with the oil and particle combination for which stable capillary foams are desired. 19
- Figure 11.** Typical foams with 5 wt% PS and 1 wt% oil within 1 hour after production. The control does not contain oil 19
- Figure 12.** Averages of at least three measured froth heights of foams created with 2.5 wt% HMDS modified silica and 1 wt% oil. The control does not contain oil. The blue bar is the average froth height for foams created with the oil and particle combination for which stable capillary foams are desired. 20
- Figure 13.** Typical foams with 2.5 wt% HMDS modified silica and 1 wt% oil within 1 hour after production. The control does not contain oil. 21

Figure 14. Foam stability results for foams produced with different oils and particles. The foams circled are combinations for which stable capillary foams are desired. A stable capillary foam would indicate that the particles adsorb strongly to the oil-water interface.	22
Figure 15. Foam containing 10 wt% PVC and 1 wt% toluene from Figure 14 after 2 weeks.	23
Figure 16. Foam stability test results for PS control with 5 wt% PS and no oil.	24
Figure 17. Deformed air bubble surrounded by DINCH and PVC particles at the DINCH-water interface.	26
Figure 18. Capillary bridging between PVC particles in foams created with DINCH and PVC.	26
Figure 19. PS aggregate that is seen throughout the recovered toluene-PS “froth.”	27
Figure 20. Multiple air bubbles stabilized with a thin layer of heptane and HMDS modified silica particles.	28
Figure 21. An air bubble stabilized by a thin layer of heptane and HMDS modified silica particles.	28
Figure 22. Heptane-HMDS modified silica and DINCH-PVC were found to be successful combinations. The toluene and PS combination was unsuccessful (as shown with the red “x” drawn over the combination).	31
Figure 23. The detachment energy, ΔE , to remove a particle from an interface increases by replacing an air-water interface with an oil-water interface.	33
Figure 24. Step-by-step pictures of the hysteresis method with an inverted sessile drop of oil. (A) A 2 μL droplet is deposited on the solid surface and the baseline is recorded. (B) The drop is grown at a rate of 0.125 $\mu\text{L/s}$ and the contact angle changes. (C) When the contact angle equals θ_{adv} , the baseline increases. (D) The droplet is then retracted at a rate of 0.125 $\mu\text{L/s}$ and the contact angle changes again. (E) Once the contact angle equals θ_{rec} , the baseline changes again. (F) Continuing retraction of the droplet will cause the droplet to become distorted and no more meaningful information can be extracted.	36
Figure 25. Typical SEM image of washed PVC particles.	38
Figure 26. Typical SEM image of washed PS particles.	38
Figure 27. Interfacial tension measurements of a pendant drop of heptane in deionized water.	40
Figure 28. Interfacial tension measurements of a pendant drop of toluene in heavy water.	41
Figure 29. Interfacial tension measurements of a pendant drop of diisononyl cyclohexane-dicarboxylate in heavy water.	41

Figure 30. Three phase contact angle as measured through the aqueous phase via the hysteresis method.	42
Figure 31. Typical particle size distribution of PVC particles.	44
Figure 32. Typical particle size distribution of PS particles.	44
Figure 33. PVC and PS particle adsorption strength to oil-water interfaces in units of $k_B T$.	45
Figure 34. Coalescence being temporarily arrested by the HMDS modified silica particle stabilized heptane-water interface of two large bubbles.	52
Figure 35. Multiple air bubbles stabilized by HMDS modified silica particles at the heptane-water interface around the bubbles.	52
Figure 36. HMDS modified silica particles stabilizing the heptane-water interface coating an air bubble.	53

LIST OF SYMBOLS

V	actual drop volume
k_B	Boltzmann constant
E	cohesive energy
R	cohesive energy ratio
ρ_i	density of component i
ΔE	detachment energy
F	geometric packing factor
γ	interfacial tension/surface energy
$LP_{c,max}$	maximum capillary pressure
d_i	middle size diameter of the i^{th} interval
\dot{V}	molar volume
A_{ij}	net interaction between the molecules of components i and j
d_n	number-average diameter
x_i	number fraction of particles in the i^{th} interval
n_i	number of particles in the i^{th} interval
r	radius
δ	solubility parameter
T	temperature
V_{max}	theoretical maximum drop volume
θ	three phase contact angle
Wo	Worthington number

LIST OF ABBREVIATIONS

CER	cohesive energy ratio
DINCH	diisononyl cyclohexanedicarboxylate
DLS	dynamic light scattering
HMDS	hexamethyldisilazane
HLB	hydrophile-lipophile balance
PDMS	polydimethylsiloxane
PS	poly(styrene-co-divinylbenzene)
PVC	poly(vinyl chloride)
SEM	scanning electron microscopy
wt%	weight percent

SUMMARY

Many applications require the selective removal of particulate contaminants from aqueous solutions. Standard froth flotation is a very efficient process that is commonly used in these applications to indiscriminately remove very hydrophobic micron-sized particulate contaminants. It is desirable to have a method that can take advantage of the efficiency of such a process and be selective with regards to what particles are removed from the solution.

Coating the air bubbles with a thin layer of oil allows for the possibility of selecting oils that have strong attractive intermolecular interactions with a targeted particle and weak attractive interactions with other particles in the solution. This could cause only the targeted particle to strongly adsorb to the oil-water interface and rise to the top of the suspension with the bubble, while the other particles remain in the suspension. Demonstrating this concept of using oil-coated air bubbles to selectively remove particulate contaminants from process effluents, called “affinity flotation,” would be novel. This study focuses on the first step required to prove affinity flotation, which is examining potential oil and particle combinations that could be used to demonstrate the idea of affinity flotation.

The main goals of this study are to (1) find three oils that can selectively remove only one particle from an aqueous suspension via one of the following attractive intermolecular interactions: hydrophobic, π - π , and acid-base; and (2) quantify the strength of the affinity the particles have for each of the possible oil-water interfaces. Potential oil and particle combinations were chosen based off the propensity of their molecular structures to have one of the aforementioned intermolecular interactions between them. These potential combinations were then screened using simple foaming ability and foam stability tests. Confocal microscopy was used to verify that capillary foams could

be made for the chosen oil and particle combinations. The strength of the affinity a particle has for an oil-water interface was determined by using data collected through measuring the oil-water interfacial tension, the three phase contact angle of a particle at the interface, and the particle size.

Results suggest that all of the oils were selective to one type of particle (i.e. only one particle had a high affinity for the oil-water interface, while the other particles had a low affinity); however, only two of the oils (DINCH and heptane) were selective towards the particles that were originally chosen because they have primarily one type of attractive intermolecular interaction with the oil (PVC via acid-base with DINCH and HMDS modified silica via hydrophobic with heptane). The other oil, toluene, was selective for PVC, but not for PS. The attractive intermolecular interactions between toluene and PS were too strong, resulting in the undesirable result of PS having a low affinity for the toluene-water interface. The calculated strength of particle adsorption to oil-water interfaces for PVC and PS particles were high for combinations that produced stable capillary foams in the foaming ability and stability tests, and low for combinations that were either semi-stable or unstable. This demonstrates why these quick and simple tests can be used to predict when particles have a high affinity for the oil-water interface of an oil-coated air bubble, and confirms that DINCH maybe selective enough to be used as an oil to demonstrate affinity flotation by removing PVC particles from binary suspensions.

In short, this study provided some progress towards developing a model system to use to demonstrate affinity flotation by finding two oil and particle combinations (DINCH-PVC and heptane-HMDS modified silica) that could potentially be used in such a system.

CHAPTER 1: INTRODUCTION

Many applications, including protein extraction¹⁻³, wastewater purification⁴⁻⁷, mineral concentration⁷⁻⁹, and recycled paper deinking^{4, 10-11}, require the selective separation of particles from aqueous suspensions. Very efficient flotation processes, like froth flotation and dissolved air flotation, are currently being used to remove micron-sized particles in many of these applications by introducing air bubbles to the solution. But, these processes are not very selective because the air-water interfaces of the bubbles only allow for the indiscriminate removal of very hydrophobic particles^{8, 12}. It is desirable to have a method that can take advantage of the benefits of these flotation processes, like high extraction efficiency, while providing the option of being highly selective in what particles will be removed.

1.1 Flotation Process Improvements

There have been many attempts to make current flotation processes more selective. Most of these attempts have been aimed at modifying the surfaces of particles to be more hydrophobic^{8, 12-16}, while other attempts have focused on modifying the air-water interface¹⁷⁻²¹.

1.1.1 Particle Surface Modifications with Promoters

A promoter is heteropolar molecule with a non-polar component and a polar component, much like a surfactant^{8, 12, 15}. When promoters are introduced to a dispersed particle system, they begin to accumulate on the solid particle surfaces and alter the hydrophobicity of the particles. In the case of more hydrophilic particles, the polar component of promoters will adsorb to their surfaces and change them to being more hydrophobic^{8, 12, 15-16, 22}. This suggests the addition of

promoters would be sufficient in a case where a very hydrophilic particle needs to be made hydrophobic enough to adsorb to the air-water interface of air bubbles in flotation columns.

However, promoters are not always very selective as they indiscriminately adsorb to particles with favorable surface chemistries^{8,12}. For example, to selectively separate feldspar from quartz, a mixture of promoters must be used at a low pH in order for the surface charges to differ enough (i.e. feldspar would be negatively charged and quartz would be neutral at $\text{pH} < \sim 2$) that only feldspar would undergo surface modification¹⁵. At higher pH values, selective separation would be impossible because the promoters would adsorb to both feldspar and quartz. Alternative methods would be needed in order to cost-effectively selectively remove particulate contaminants from aqueous effluents in the case of a promoter, or a mixture of promoters, adsorbing to more than just the contaminant particles.

1.1.2 Oil-Coated Air Bubbles for Particle Separation

A potentially less invasive method to selectively remove particulate contaminants from aqueous solutions would be to use a thin layer of oil to coat an air bubble in order to change the interface the particles interact with from an air-water interface to an oil-water interface. This allows for the possibility of choosing only oils that will strongly interact with a small number of particles and, hence, only allowing for the selective adsorption of a particular contaminant particle to the oil-water interface. This idea has been proposed as early as 1927, when Taggart suggested that this could enhance flotation performance by allowing for the adsorption of less hydrophobic particles²³. In the recent decade, some work has been centered around this idea and applied to processes such as bitumen recovery¹⁷⁻¹⁸, solvent extraction¹⁹⁻²⁰, and recycled paper deinking²¹. These studies have focused more so on the application of this idea rather than some of the more fundamental aspects.

As a result, the Behrens and Meredith groups have recently focused on examining bubble dynamics and interactions between particles and oil-coated bubbles²⁴⁻²⁹. They have proven that particles can help oils wet the air-water interface and that very stable foams can be created using oil-coated bubbles and particles with the right wettability^{24-25, 28}. Also, the oil-coated bubbles rise more slowly in the aqueous solution than standard air bubbles, which means there is more time for a particle to interact with the oil-water interface; thus, increasing the likelihood of a target particle adsorbing to the interface²⁹. These results suggest oil-coated bubbles might be useful for selectively removing particles from aqueous suspensions, but more work needs to be done in order to prove this.

1.2 Objective

This work focused on the first step required to build a model system to demonstrate the concept, called “affinity flotation,” of using oil-coated air bubbles to selectively remove particles from binary particle suspensions via attractive intermolecular interactions, such as π - π , acid-base, and hydrophobic interactions. This first step has been split into two parts. First, oil and particle combinations were chosen using simple foaming ability and stability tests to screen the potential pairings. Next, the strength of the particle adsorption to the oil-water interface was quantified for each possible oil and particle combination. These steps will ideally provide the information required to demonstrate, for the first time, the selective removal of particles from aqueous suspensions via intermolecular interactions with oil-coated bubbles.

CHAPTER 2: OIL-PARTICLE INTERACTIONS AND FOAM FORMATION

2.1 Overview

The goal of this chapter is to find three pairs of oils and particles that could potentially be used in a model system to demonstrate affinity flotation. Oil and particle combinations were initially selected on the basis of the potential of the oil and particle molecular structures to have one of the following attractive interactions between them: acid-base, hydrophobic, and π - π . The selected combinations were screened using simple foaming ability and foam stability tests. A successful pairing (for the purpose of demonstrating selectivity) is one in which the oil is selective to only one particle type (i.e. only the particle expected to have strong attractive intermolecular interactions with the oil has a strong affinity for the oil-water interface, while other particles have a weak affinity) as shown in Figure 1. If a stable froth is produced with an oil and particle pairing during the foaming ability and foam stability tests, then the particle has a strong affinity for the oil-water interface. If semi-stable or unstable froths are produced, then the particle affinity for the oil-water interface is unknown and must be determined quantitatively.

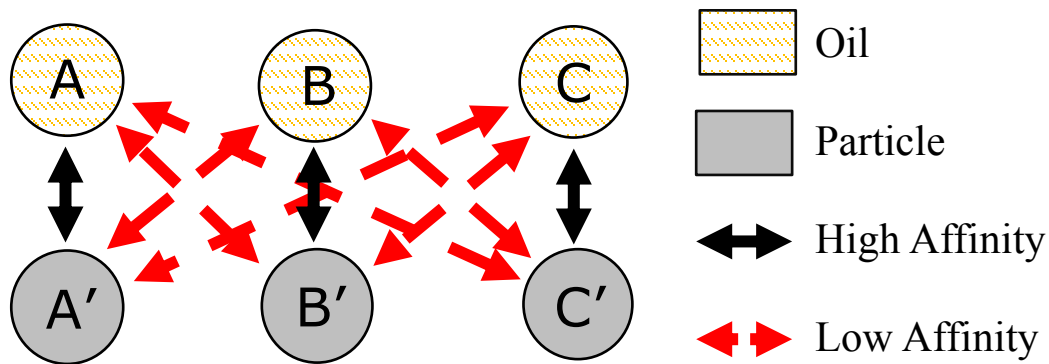


Figure 1. Diagram showing the requirements for successful oil and particle combinations.

2.2 Background and Theory

Just like with other liquid-liquid-solid systems, such as those found in Pickering emulsions³⁰⁻³², bicontinuous interfacially jammed emulsion gels (bijels)³³⁻³⁶, and capillary foams^{24-25, 28}, the particle wettability is crucial for determining whether or not a particle adsorbs and remains at the oil-water interface. The Young equation is commonly referenced when discussing the wettability of particles at the interface of two fluids and, for an oil droplet on a solid surface under water as depicted in Figure 2, is³⁷⁻³⁸

$$\gamma_{OW}\cos\theta = \gamma_{SO} - \gamma_{SW} \quad (1)$$

where θ is the three phase contact angle measured through the aqueous phase and γ_{ij} is the interfacial tension of the interface formed by phase i and phase j .

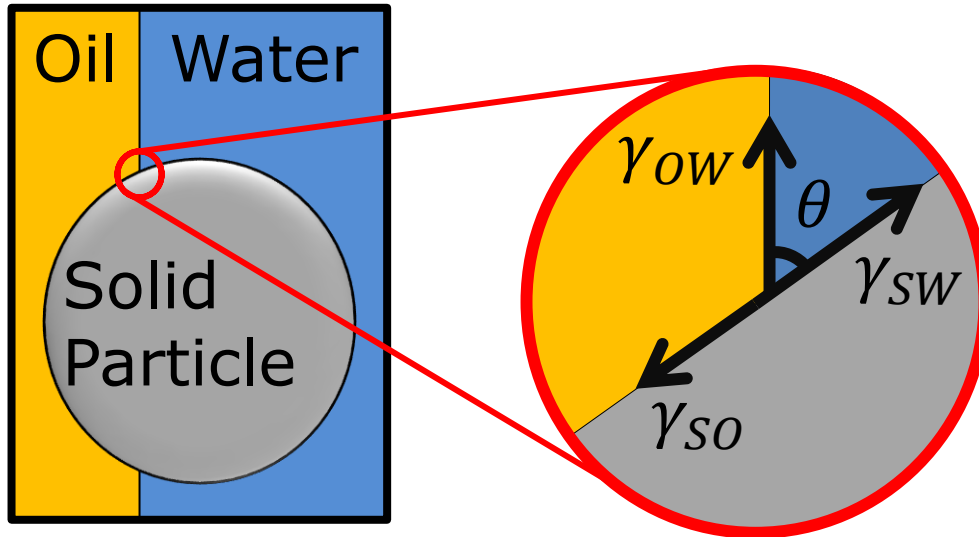


Figure 2. Example showing the location of the three phase contact angle and the directions of the interfacial tensions of each interface.

Interfacial tension is the surface energy per unit area of an interface between two phases and heavily depends on the interactions between the phases. The stronger the attractive interactions are between two phases, the lower the interfacial tension. So, if the intermolecular attractive

interaction strength between the solid and the oil in Figure 2 increases (i.e. γ_{SO} decreases) while it remains the same for interactions across the water-solid and oil-water interfaces, then the three phase contact angle would have to increase in order for the Young equation to be satisfied. In reality, it is extremely difficult to change only one of the surface energies without changing one of the other two. For example, in the previously described scenario, the solid surface or the oil would have been modified, which would lead to changes in at least one of the other surface energies (just γ_{OW} for changes to the oil and both for changes to the solid surface). Furthermore, changes to the oil would affect the intermolecular interactions between the oil molecules themselves, which would cause γ_{OW} and γ_{SO} to either increase or decrease depending on whether the intermolecular interactions between the oil molecules become more attractive or repulsive respectively. A similar result can be realized for changes to the solid surface, with intermolecular interactions between surface functional groups affecting the interfacial tension between the solid surface and the liquid phases. So, the intermolecular interactions between each phase as well as those within each phase in systems dealing with particles at liquid-liquid interfaces are very important to consider.

The same is true in systems with particles at gas-liquid interfaces, such as Pickering foams. Pickering foams were first discovered by Ramsden³⁹ in 1903, but their discovery has usually been attributed to Pickering, who observed the same phenomenon four years later and even referenced Ramsden⁴⁰. In Pickering foams, solid particles adsorb to the air-water interfaces of air bubbles and rise to the top of the aqueous suspension to form a froth that can be much more stable than surfactant stabilized foams⁴¹. This type of stability arises from the high energy associated with colloidal-size particles attaching to the air-water interface. This energy can be quantified as the detachment energy or the energy required to remove a particle from an interface. Equation 2 shows

the detachment energy, ΔE , required to remove a particle of radius r from an air-water interface into the aqueous phase⁴²⁻⁴³.

$$\Delta E = \pi r^2 \gamma_{AW} (1 - |\cos \theta|)^2 \quad (2)$$

Where γ_{AW} is the surface tension of water. For colloidal-sized particles of the appropriate wettability, this energy can be in the hundreds of thousands $k_B T$, which is large enough to overcome thermal and mechanical energy being transmitted by various sources as the air bubble rises in the solution⁴¹. This means the particle adsorption to the interface is essentially irreversible and, once enough particles adsorb to the interface and a froth is created, the particles enhance the stability of the froth by limiting bubble coalescence and Ostwald ripening^{38, 42}. Creating Pickering foams with this type of stability is achievable with hydrophobic particles; however, many water dispersible particles are very hydrophilic and do not have the right wettability to adsorb strongly to the air-water interface.

Many of these types of particles have better wettability with certain oil-water interfaces than air-water interfaces (i.e. their contact angles are between 50° and 130° at an oil-water interface as opposed to $< 50^\circ$ at an air-water interface). This means they can stabilize oil-coated air bubbles in a so-called capillary foam discovered by the Behrens and Meredith groups^{24-25, 28}. Figure 3 shows a schematic of what a capillary foam is thought to look like. A capillary foam is thought to consist of two main parts: air bubbles coated with oil stabilized by particles at the oil-water interface and a particle-particle capillary bridge network extending throughout the aqueous phase and connecting with the bubbles. To produce these foams, a very small amount (< 2 wt%) of oil is added to an aqueous particle suspension followed by vigorous agitation^{24-25, 28}. It is important to note that these capillary foams are not expected to be the same as the types of foams created in

affinity flotation. The primary reason for this expectation is the foams are produced in different ways. In capillary foams, the small amount of oil is directly added to the aqueous particle suspension and foams might be created upon vigorous agitation. In affinity flotation, the oil is introduced to the aqueous particle suspension via air bubbles. Foams may not actually be created in affinity flotation, but the particles just need to be consolidated at the top of the aqueous suspension in order for them to be successfully removed. Regardless, particles must have a strong affinity for the oil-water interface in order for a stable foam to be created (for capillary foams)^{24-25, 28} or for particles to end up at the top of an aqueous particle suspension (for affinity flotation).

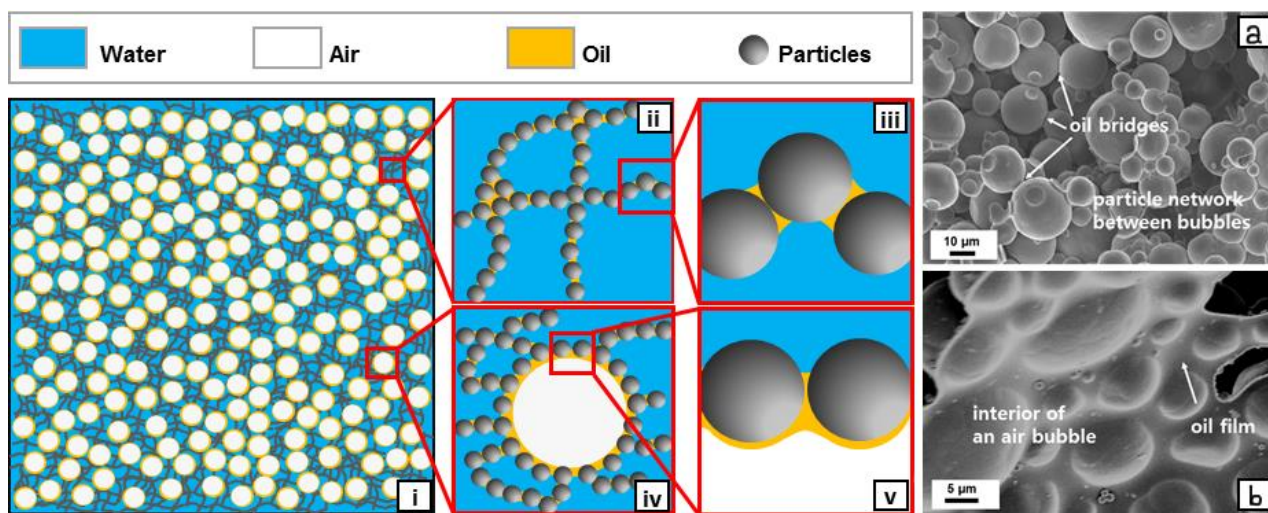


Figure 3. Left: Proposed structure of capillary foams (i). The system contains a continuous liquid phase (Water), a vapor phase (Air), a secondary fluid phase (Oil), and a solid phase (Particles). The solid particles should have a high affinity to the Water/Oil interface. Choosing the right composition of the four components and agitating the mixture yields a space-spanning network of particles in water (ii) connected by bridges of oil (iii), with bubbles of air embedded in the network (iv) via a stabilizing hybrid coating of oil and particles (v), adapted with permission from Zhang et al²⁸. Copyright 2014 American Chemical Society. Right: Scanning electron microscopy images of oil-bridged particles (a) and bubble coating in a capillary foam (b), taken with permission from Zhang et al²⁴.

So, if oil-coated air bubbles are used to remove one type of particle from a binary particle suspension, then one particle must have a strong affinity for the oil-water interface (i.e. contact angle near 90°), while the other must have a weak affinity for the interface (i.e. contact angle far

from 90°). The only way to adjust the affinity without adding substances, such as salt, to the aqueous phase in this case would be to adjust the oil phase such that it has stronger intermolecular interactions with the targeted particle than with the non-targeted one. Changing the oil phase instead of adding additives to the aqueous phase has two primary benefits: (1) changing the oil phase can have a stronger effect on the particle wettability than additives would and (2) changing the oil can be more practical, as it already consists of a very small fraction of the overall system. Probing these oil-particle interactions could be useful in identifying potential oils that can be used to effectively remove solely the targeted particles.

2.3 Oil and Particle Selection

Hildebrand first used the term “solubility parameter” in the mid-twentieth century⁴⁴. The solubility parameter of a substance, δ , is defined as the square root of its cohesive energy, E , over its molar volume⁴⁵. When written out, this becomes

$$\delta = \sqrt{\frac{E}{\dot{V}}} \quad (3)$$

where \dot{V} is the molar volume.

The cohesive energy is directly related to the heat of vaporization of a substance and dividing this term by the molar volume is called the cohesive energy density, which is essentially a measure of the magnitude of the intermolecular forces within the substance⁴⁶⁻⁴⁸. So, if an oil and a particle have similar solubility parameters, then strong attractive intermolecular interactions will exist between them. It would be great to use solubility parameters to identify potential oil and particle combinations, but there is one problem. For a particle to have a strong affinity for the *oil-water interface*, the particle would need to be nearly equally wetted by both the oil and the water.

A particle that is wetted too easily by the oil may end up in the oil phase instead of the interface. Add to this the fact that the geometry of the particle as well as the interactions between the oil and the water affect the strength of particle adsorption to the oil-water interface, and this suddenly becomes a very complex system. Is there a theory that relates the solubility parameter to the three phase contact angle or even the solid-liquid interfacial tension value?

In the literature, the solubility parameter has been used to predict what types of non-ionic surfactants could strongly adsorb to a fluid-fluid interface. Beerbower and Hill developed the “cohesive energy ratio” (CER) concept for the stabilization of emulsions with non-ionic surfactants⁴⁹. This concept makes the following assumptions⁵⁰: (1) both moieties of the surfactant match chemically with their respective preferred phase (i.e. the hydrophobic moiety matches the oil and the hydrophilic moiety matches water), (2) the solubility parameter of the hydrophobic tail is equal to that of the oil and likewise for the solubility parameters of the hydrophilic head and water, (3) the molar volume of the lipophilic tail is equal to that of the oil and likewise for the molar volumes of the hydrophilic head and water, and (4) the hydrophile-lipophile balance (HLB) is defined using Griffin’s method. These assumptions allow for the possibility of combining Winsor’s R ratio with Griffin’s HLB concept, which results in⁵⁰

$$R = \frac{\rho_H}{\rho_L} \left(\frac{20}{HLB} - 1 \right) \frac{\delta_L^2}{\delta_H^2} \quad (4)$$

where ρ_i is the density of component i , R is the cohesive energy ratio, the lipophilic tail of the surfactant is denoted as L , and the hydrophilic head of the surfactant is denoted as H . Note that Winsor’s R ratio can also be written in terms of net interactions⁵¹, as shown in Equation 5.

$$R = \frac{A_{SO} - A_{OO}}{A_{SW} - A_{WW}} \quad (5)$$

Where A_{SO} and A_{SW} are the net interaction of surfactant molecules per unit area at the interface with the oil and water respectively, and A_{ii} is the net interaction between two molecules of liquid i . This means that when $R < 1$, the system would favor the formation of an oil-in-water emulsion. And when $R > 1$, a water-in-oil emulsion is preferred⁵⁰⁻⁵¹. Figure 4 shows a schematic of these two cases as well as the preferred state when $R = 1$.

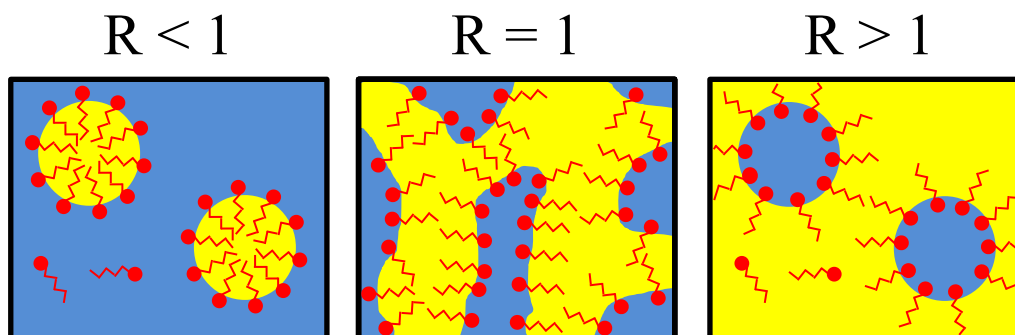


Figure 4. The preferred emulsion types based on Winsor's R ratio. The preferred emulsion when $R = 1$ is a bicontinuous structure microemulsion.

With this in mind, Equation 4 can be used to either predict what type of non-ionic surfactant is needed to obtain a particular R value or to predict what type of emulsion would form for a known non-ionic surfactant. This has been done to predict what types of surfactants can be used in emulsion polymerization, but how this concept could be extended to Pickering emulsions is still unclear^{50, 52-53}.

In light of this, the selection of oils and particles with potentially strong intermolecular interactions was done on the basis of the propensity of their molecular structures to have primarily one of the following intermolecular interactions: hydrophobic, π - π , and acid-base. π - π interactions occur between two π -systems when the attractive interactions between π -electrons and the positively charged σ -framework are greater than the repulsive interactions between π -electrons⁵⁴. An attempt to exploit these interactions was made by using toluene as the oil and poly(styrene-co-

divinylbenzene) (PS) as the particle. Acid-base interactions involve interactions between Lewis acid electron acceptors and Lewis base electron donors. Poly(vinyl chloride) (PVC) was chosen as a Lewis acid particle due to its possibly weak acid properties⁵⁵⁻⁵⁶, while diisononyl cyclohexanedicarboxylate (DINCH) was chosen to be a Lewis base oil due to the potential of the carboxylate groups driving the molecule to be more of an electron donor. Hydrophobic interactions involve interactions between two more nonpolar components surrounded by a more polar medium and are driven by thermodynamically favorable state of the two components aggregating to minimize solvation free energy⁵⁷. These interactions were exploited using hexamethyldisilazane (HMDS) modified silica particles and heptane. Figure 5 shows the molecular structures of each oil and particle.

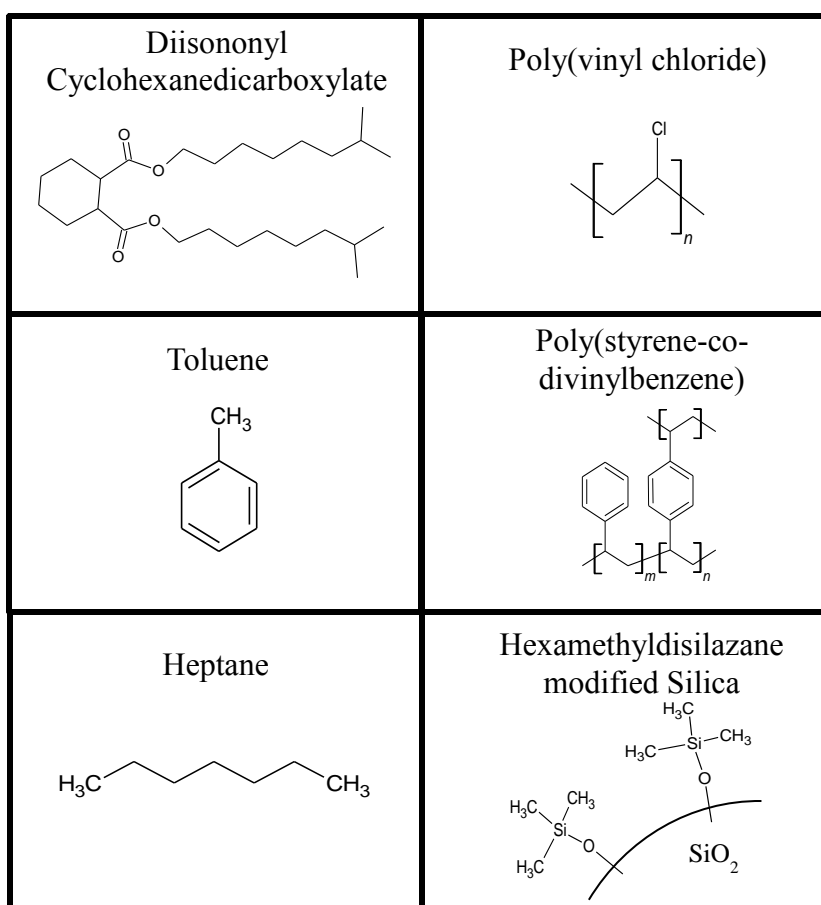


Figure 5. All the oils (left column) and particles (right column) used.

2.4 Methods

The solid particles used are Vinnolit SA 1062/7 poly(vinyl chloride) (PVC) particles obtained from Vinnolit, poly(styrene-co-divinylbenzene) (PS) microspheres obtained from Sigma Aldrich, and AEROSIL[®] R 812 S hexamethyldisilazane (HMDS) modified silica particles obtained from Evonik. The PVC particles were washed with deionized water several times before being used. Both the PS and HMDS modified silica particles could not be readily dispersed in deionized water because of their high hydrophobicity due to the entrapment of air in their pores (gaps between aggregated HMDS modified silica particles⁵⁸ and possibly nanopores on the PS surfaces⁵⁹) that lead to Cassie-Baxter wetting⁶⁰⁻⁶². To displace the air, the particles were dispersed in acetone and rinsed several times with deionized water.

The oils used are heptane, toluene, and DINCH. The heptane and toluene were obtained from Sigma Aldrich, while the DINCH was obtained from TCI America. All oils were purified using silica gel obtained from Sigma Aldrich.

2.4.1 Foam Production

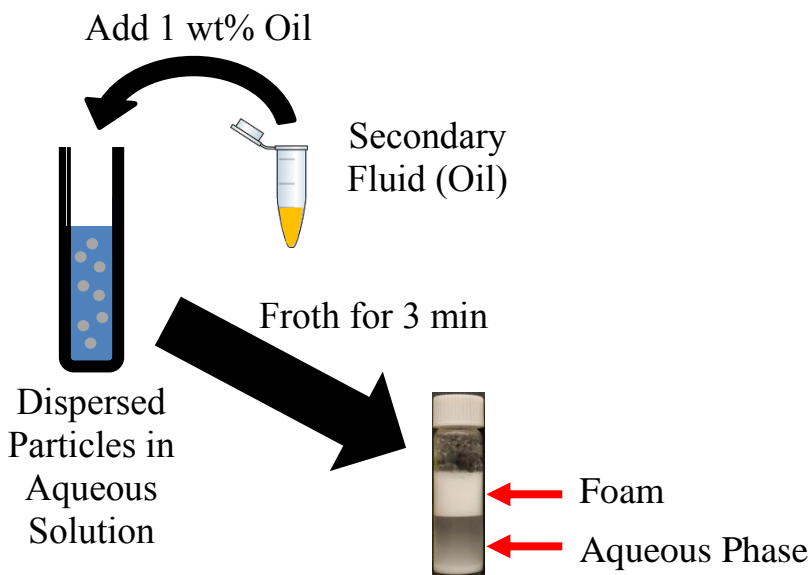


Figure 6. Diagram of the procedure used to create foams for foaming ability and foam stability tests.

All foams were produced with the following procedure, which is depicted in Figure 6. First, particles were dispersed by agitating the aqueous solution with a vortex mixer (Scientific Industries Vortex-Genie 2) on the highest setting for 15 seconds. If HMDS modified silica particles were used, then the solution was also sonicated for 15 minutes using a VWR sonicator. Second, a small amount (1 wt%) of oil was added to the solution. For Pickering foams, this second step was skipped. Finally, the solutions were vigorously mixed for 3 minutes with a IKA Ultra-Turrax T10 homogenizer at 30,000 rpm to create foams.

2.4.2 Foam Properties

Two simple tests were performed to qualitatively estimate when a particle has a strong affinity for an oil-water interface: foaming ability and foam stability. Foaming ability tests were used to qualitatively determine the possibility of foams being created using a certain particle to stabilize the oil-water interface surrounding an air bubble. Foam stability tests provided more concrete evidence on the affinity a particle has for an oil-water interface.

2.4.2.1 Foaming Ability Tests

Foaming ability tests were performed to determine the height of the foams immediately after creation. After a foam was produced, the froth height was determined using a ruler. Foam buildup along the sides of the glass vial were not accounted for in the froth height measurements; instead, the froth height was measured by measuring the distance between the lowest points of the top and bottom of the froth as shown in Figure 7.

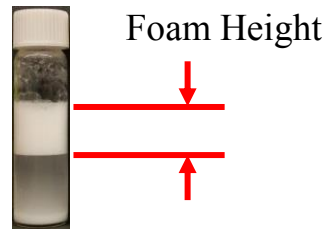


Figure 7. Example of how froth height is determined.

2.4.2.2 Foam Stability Tests

An important aspect of the stability of particle stabilized foams is the capillary pressure of the thin film between air bubbles. This is more important after a foam has been created and most of the liquid has either evaporated or drained out of the foam. The film will rupture once the pressure inside of the film exceeds the maximum capillary pressure, $P_{c,max}$, which, bubbles stabilized with a single layer of particles, is defined as⁶³

$$P_{c,max} = F \frac{2\gamma \cos\theta}{r} \quad (6)$$

where F is a geometric parameter reflecting the particle packing in the film, r is the particle radius, and γ is the interfacial tension of the interface the particles stabilize. The greater the maximum capillary pressure is, the better the foam stability.

In this work, foams had their resistance to destabilization mechanisms, such as coalescence and Ostwald ripening, determined by leaving them in a quiescent state and checking them daily until the froths completely dissipated. Images of the foams were taken on a daily basis until the foams completely collapsed.

2.4.3 *Confocal Microscopy*

Confocal microscopy was used to verify that suspected foams were actual foams and not particle aggregates that cream at the top of the aqueous solution. In confocal microscopy, the locations of fluorescent probes are imaged. These probes can be molecules of interest, like fluorescent surfactants, or they can be fluorescent dyes dissolved in a liquid phase⁶⁴. When valance electrons within the fluorescent molecules are excited with light of a certain wavelength, they jump to a higher energy state. Once the excited electrons relax back to the ground state, they release energy in the form of visible light.

In imaging the foams in this study, a florescent dye was used to dye the oil phase. This dye, Nile Red, was obtained and used as received from Sigma-Aldrich. For each of the oils, 0.74 mg of Nile Red was added per g of oil, which is small enough that it can be assumed the interfacial properties of the oil will not be affected. The amount of dyed oil added to these foams was twice as much as the 1 wt% used to create foams for the foaming ability and foam stability tests. This was done to ensure enough oil would be present to see oil coating air bubbles. The foams were imaged using an Olympus FV1000 confocal microscope (excitation at 543 nm and emission above 560 nm) and analyzed with ImageJ.

2.5 Results

2.5.1 Foaming Ability

2.5.1.1 Foams with PVC

Figure 8 shows the froth heights of foams created with 10 wt% PVC and 1 wt% oil, while Figure 9 shows images of foams taken within 1 hour after frothing.

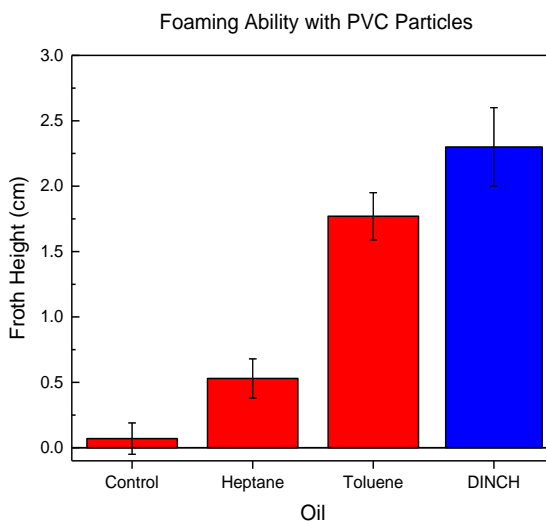


Figure 8. Averages of at least three measured froth heights of foams created with 10 wt% PVC and 1 wt% oil. The control does not contain oil. The blue bar is the average froth height for foams created with the oil and particle combination for which stable capillary foams are desired.

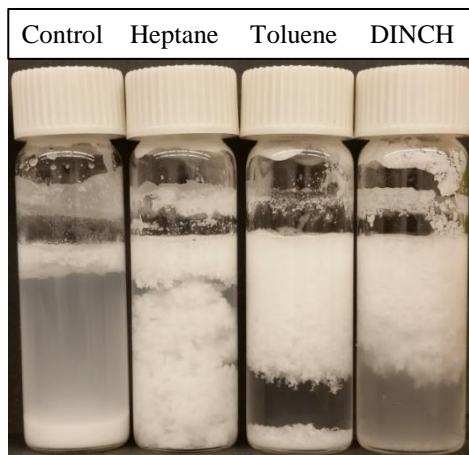


Figure 9. Typical foams with 10 wt% PVC and 1 wt% oil within 1 hour after production. The control does not contain oil.

The average foam height of the Pickering foams produced with these particles was close to zero. According to Zhang et al., these particles do not strongly adsorb to an air-water interface and, thus, should not produce a foam, which explains why the froth height was so low²⁴. Adding an oil phase to coat the air bubbles resulted in the PVC particles ending up in an apparent froth at the top of the aqueous solution independent of the oil used. When heptane was used as the oil phase, a small froth was produced at the top of the aqueous phase with a large capillary suspension below it in the aqueous phase. This suggests the PVC particles do not have a wettability that allows them to strongly favor stabilizing the oil-water interface of an oil-coated air bubble, meaning the three phase contact angle is too far from 90°. When the polar and basic oils (toluene and DINCH) were added to the system, more froth was produced than when the neutral, nonpolar oil of heptane was added, indicating that the possible stronger interactions between slightly acidic PVC and the basic, polar oils could be driving the increase in foam volume by allowing for stronger adsorption of PVC to the oil-water interface. The experiments performed in Chapter 3 of this thesis will address the particle adsorption affinity. Furthermore, it must be stressed that these foaming ability tests also do not prove that an actual foam has been produced. Microscopy and, in some cases, foaming stability tests will yield more information on whether or not a foam actually was produced.

2.5.1.2 Foams with PS

On the next page, Figure 10 shows the froth heights of foams created with 5 wt% PS and 1 wt% oil, while Figure 11 shows images of foams taken within 1 hour after frothing.

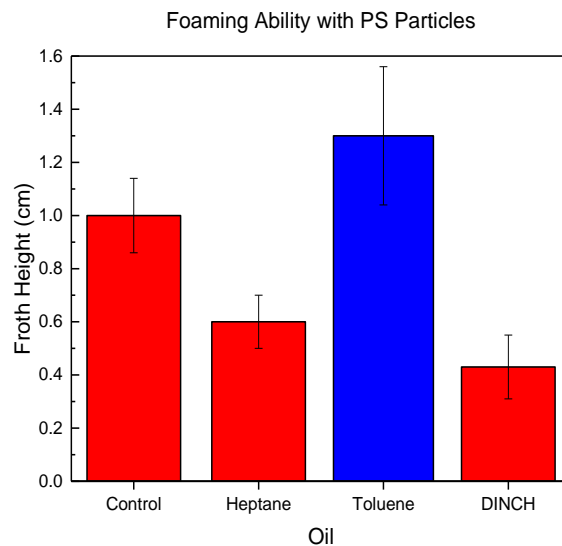


Figure 10. Averages of at least three measured froth heights of foams created with 5 wt% PS and 1 wt% oil. The control does not contain oil. The blue bar is the average froth height for foams created with the oil and particle combination for which stable capillary foams are desired.

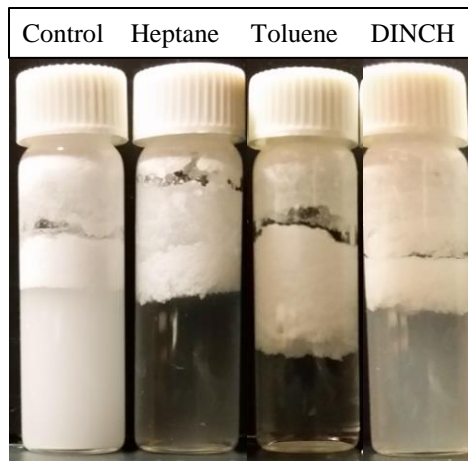


Figure 11. Typical foams with 5 wt% PS and 1 wt% oil within 1 hour after production. The control does not contain oil. A thin layer of particles coat the insides of the vials above the apparent froths.

These hydrophobic particles appear to have a propensity to adsorb to the air-water interface, as the attempts to produce Pickering foams proved successful. Adding oil to the system produced varying results. Adding heptane or DINCH to the system produced foams with poorer foaming ability than the Pickering foams. A larger apparent foam was created using toluene to coat air bubbles, compared to those made with DINCH, heptane, and no oil at all. Of the three oils, the

PS particles are expected to interact most strongly with toluene because of its ability to participate in π - π interactions such as π - π stacking. These foaming ability results suggest that more particles will end up at the top of the suspension when toluene is introduced as the oil to coat air bubbles. It is not clear whether or not these are actually foams from the foaming ability tests alone.

2.5.1.3 Foams with HMDS Modified Silica

Figure 12 shows the froth heights of foams created with 2.5 wt% HMDS modified silica and 1 wt% oil, while Figure 13 on the next page shows images of foams taken within 1 hour after frothing.

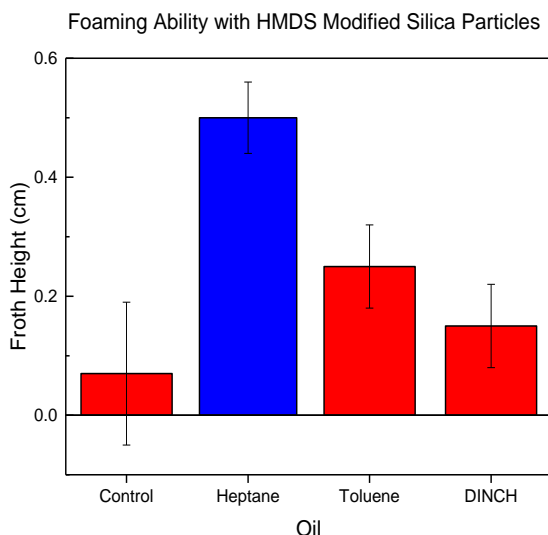


Figure 12. Averages of at least three measured froth heights of foams created with 2.5 wt% HMDS modified silica and 1 wt% oil. The control does not contain oil. The blue bar is the average froth height for foams created with the oil and particle combination for which stable capillary foams are desired.

Attempts to create a Pickering foam did not appear to be successful, as hardly any froth formation was observed. This suggests that the HMDS modified silica particles either do not stabilize the air-water interface or could overcome the barrier to adsorption to an air-water interface due to the low particle concentration⁶⁵. Adding polar oils, like DINCH and toluene, to the system provides little to no improvement in the foaming ability as their froth heights were comparable to

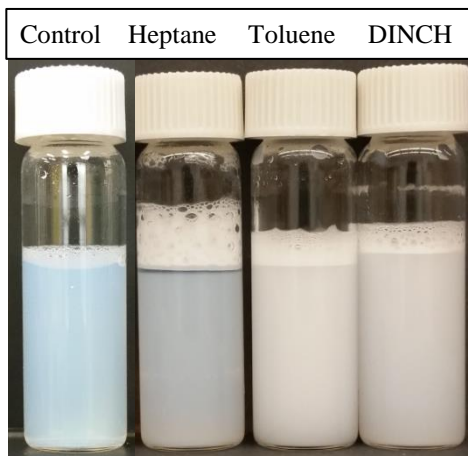


Figure 13. Typical foams with 2.5 wt% HMDS modified silica and 1 wt% oil within 1 hour after production. The control does not contain oil.

the froth height of the Pickering foam. However, adding a nonpolar oil, like heptane, caused a noticeable increase in the foaming ability. These particles were expected to interact well with heptane via hydrophobic interactions and these interactions could possibly lead to more particles adsorbing to the heptane-water interface and ultimately increasing the foam volume. The present foaming ability tests support this expectation, but a more rigorous verification is still desirable.

2.5.2 *Foam Stability*

Long term stability tests of the samples for each possible oil and particle pairing are shown in Figure 14 on the next page.



















Particle Type	PVC	PS	HMDS	PVC	PS	HMDS
Particle wt%	10%	5%	2.5%	10%	2.5%	
1 wt% Heptane						
	0 hr	0 hr	0 hr	1 wk	4 wks	5 wks
1 wt% Toluene						
	0 hr	0 hr	0 hr	4 mos	4 wks	1 day
1 wt% DINCH						
	0 hr	0 hr	0 hr	4 wks	4 wks	3 wks

Figure 14. Foam stability results for foams produced with different oils and particles. The foams circled are combinations for which stable capillary foams are desired. A stable capillary foam would indicate that the particles adsorb strongly to the oil-water interface.

2.5.2.1 Foams with PVC

The results of the foam stability tests for the Pickering foam and the foam created with heptane suggest the foams were very unstable if any was produced at all. The heptane system, in particular, appeared to contain a larger volume of a capillary suspension than a foam and the part

of the system near the top initially did not withstand the forces of gravity well after a week, which suggests this does not contain much of a vapor phase. So, as expected, PVC particles may not form Pickering foams, and these particles only create an unstable foam when frothed with heptane, which is a desirable outcome because PVC was selected as a potential particle to have strong attractive interactions with DINCH and not heptane.

The foams created with toluene and DINCH lasted much longer. The toluene-PVC foams were shown to last approximately 4 months, which is indicative of good stability, and were also shown to be actual capillary foams as one of the stages the foams go through in the destabilizing process shows air bubbles surrounded by particles (see Figure 15). Since Pickering foams cannot be created with these particles, it is clear the addition of the oil creates an oil-water interface that is more favorable for these particles to adsorb to.

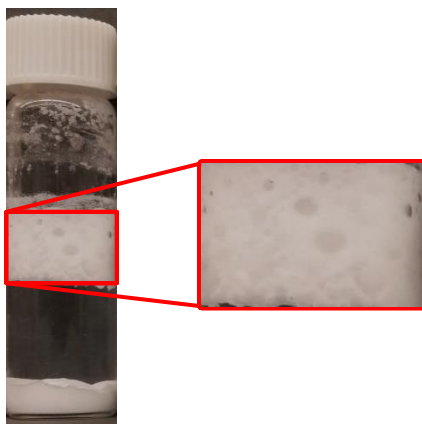


Figure 15. Foam containing 10 wt% PVC and 1 wt% toluene from Figure 14 after 2 weeks.

The long term stability of the DINCH-PVC foams is still being monitored and can be compared to the stability of the toluene-PVC foams if they last at least 3 months. If the foam lasts longer than the toluene-PVC foam, then it is possible that the PVC particles adsorb more favorably to the DINCH-water interface than to the toluene-water interface. As of now, these tests suggest stable capillary foams can be obtained with either toluene or DINCH as the oil. A stable DINCH-

PVC capillary foam is desirable, but a stable toluene-PVC foam is not. Stable capillary foams can only be created if the particles have a strong affinity for the oil-water interface, which means these results suggest PVC has a high affinity for both the DINCH-water and toluene-water interfaces. More will need to be done to quantify the adsorption strength PVC has for both interfaces. Those results may suggest that it is possible to tune the selectivity of an oil by lowering the adsorption strength of PVC to the oil-water interface. If the PVC particles have a high affinity for an oil-water interface and have a contact angle approximately 30° away from 90° , then modifications to the system can be made, such as adding surfactants to the oil phase, to lower the detachment energy. This would be useful in making toluene more selective if it were to be used as an oil to remove particles it has primarily attractive π - π interactions with from a binary suspension of such a particle and PVC.

2.5.2.2 Foams with PS



Figure 16. Foam stability test results for PS control with 5 wt% PS and no oil.

All samples, including the one made without oil (Figure 16), did not exhibit significant changes after 4 weeks. Complicating the results of these tests is the inherent hydrophobicity of the PS particles themselves. As the froth collapses, the particles could return to their initial state of

being too hydrophobic to easily return to the aqueous phase due to entrained air. This causes the particles, which are close in density to water (assuming their density is 1.05 g/mL, which is that of polystyrene⁶⁶), to cream at the top instead of settling at the bottom of the aqueous phase. Of course, this assumes these apparent foam heads are actual froths. The results from the confocal microscopy performed on the foams created with toluene suggest that these are not capillary foams and are, instead, particle aggregates that cream at the top of the aqueous solution. This is not a desirable result because the PS particles do not seem to have a high affinity to the toluene-water interface and prefer to be in the oil phase instead.

2.5.2.3 Foams with HMDS Modified Silica

For the systems with either toluene or DINCH, the results prove that the addition of either oil to the system does not create stable froths with HMDS modified silica particles. These outcomes are desirable as HMDS modified silica was chosen for its propensity to interact strongly with heptane via hydrophobic interactions, not toluene or DINCH. As for the froth created with heptane, which displayed good foaming ability, foam destabilization via coalescence and film drainage, significantly decreased the froth height over the course of 4 weeks. So, capillary foams created with heptane and HMDS modified silica particles have good stability. This is a desirable result because it means the HMDS modified silica particles adsorb strongly to the heptane-water interface.

2.5.3 Confocal Microscopy

Results from the foaming ability and foam stability tests suggest stable foams can be created for each of the chosen oil and particle combinations. To confirm that these combinations

(DINCH-PVC, toluene-PS, and heptane-HMDS modified silica) actually produce capillary foams, confocal microscopy was performed on samples of each foam.

2.5.3.1 DINCH and PVC

Figure 17 shows a deformed air bubble that was coated with oil and stabilized with particles at the oil-water interface, while Figure 18 shows evidence of capillary bridging taking place between particles, which is characteristic of capillary foams.

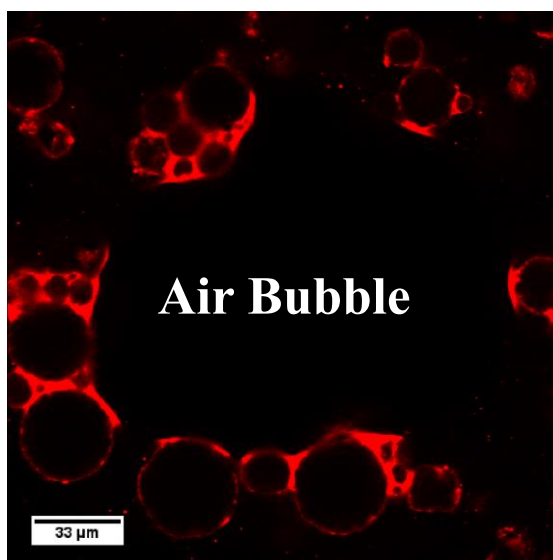


Figure 17. Deformed air bubble surrounded by DINCH and PVC particles at the DINCH-water interface.

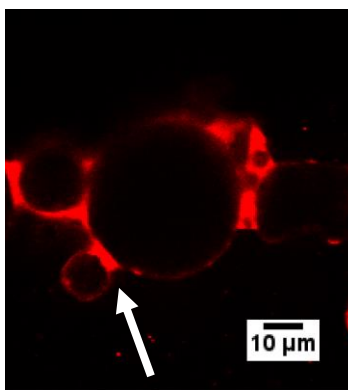


Figure 18. Capillary bridging between PVC particles in foams created with DINCH and PVC.

These images prove that a capillary foam is indeed formed when a small amount of DINCH is added and vigorously agitated with an aqueous PVC suspension, which is the desirable outcome for this oil and particle combination.

2.5.3.2 Toluene and PS

Figure 19 shows what was typically observed with the suspected foams made with toluene and PS.

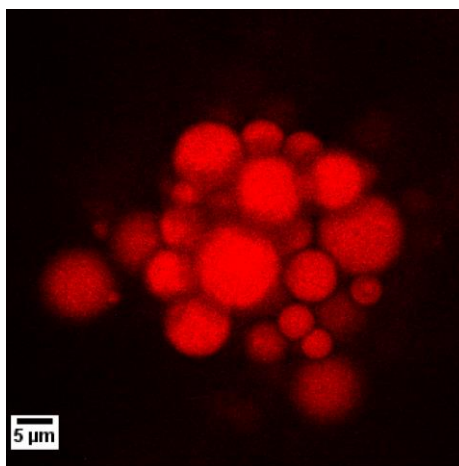


Figure 19. PS aggregate that is seen throughout the recovered toluene-PS “froth.”

The image shows that the particles just adsorb the oil and aggregate into flocs. This is not particularly surprising because these types of heavily crosslinked particles are well known to be good hydrophobic adsorbents for organic molecules in aqueous solutions⁶⁷. The hope in this case was the particles would have enough crosslinking that they would not be very susceptible to swelling and, thus, would not adsorb too much of the toluene. This would leave some toluene behind to coat an air bubble and provide an oil-water interface for the particles to adsorb to. The confocal microscopy results show that this did not happen; however, as an unfavorable result was obtained.

2.5.3.3 Heptane and HMDS Modified Silica

Figure 20 shows multiple air bubbles stabilized with HMDS modified silica nanoparticles and a thin layer of heptane, while Figure 21 shows an image at a higher magnification of a single air bubble stabilized with HMDS modified silica nanoparticles and a thin layer of heptane. More images can be found in Appendix A.

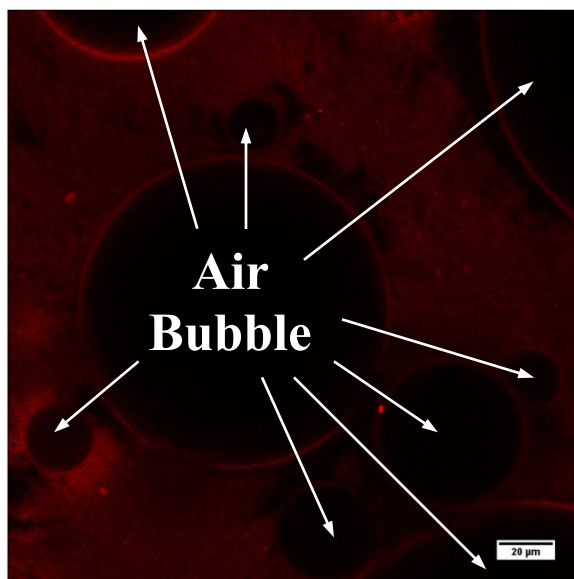


Figure 20. Multiple air bubbles stabilized with a thin layer of heptane and HMDS modified silica particles.

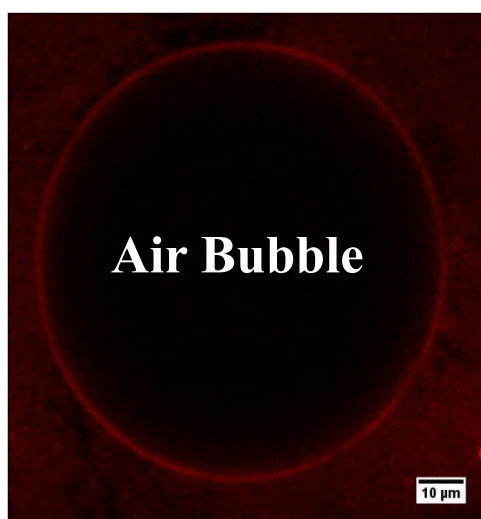


Figure 21. An air bubble stabilized by a thin layer of heptane and HMDS modified silica particles.

These images show that the foam produced with heptane and HMDS modified silica is actually a capillary foam with multiple air bubbles coated with oils and particles at the oil-water interface, which is a desirable outcome for this oil and particle combination.

2.6 Concluding Remarks

The goal of this Chapter was to find three oil and particle combinations, such that each oil is selective to only one type of particle (the particle paired with the oil has a high affinity for the oil-water interface, while the other particles have a low affinity for the interface), chosen on the basis of their potential to have primarily one attractive intermolecular interaction between them: hydrophobic, π - π , and acid-base. Simple foaming ability and foam stability tests initially screened potential combinations. Oil and particle combinations can only produce stable capillary foams if the particles have a high affinity for the oil-water interface. The affinity a particle has for an oil-water interface is unknown if the froth produced is semi-stable or unstable. Therefore, each chosen oil and particle pairing should produce stable capillary foams.

During the foam stability tests, one oil and particle combination (toluene-PVC) was confirmed to be an actual capillary foam as bubbles stabilized with particles could be seen growing larger as coalescence and Ostwald ripening continued to destabilize the froth. Since Pickering foams could not be created with the PVC particles, these foams were capillary foams, which suggests that PVC particles stabilize the toluene-water interface of an air bubble engulfed in toluene. Thus, PVC has a high affinity for the toluene-water interface, which is not desirable because PS was chosen to be the particle to have a high affinity for the toluene-water interface due to its propensity to have strong attractive π - π interactions.

Confocal microscopy was performed to verify that capillary foams were formed for each of the three oil and particle combinations chosen because they could have strong attractive interactions between them: DINCH-PVC (selected for primarily acid-base interactions), toluene-PS (selected for π - π interactions), and heptane-HMDS modified silica (selected for hydrophobic interactions). These experiments verified the presence of oil-coated bubbles stabilized by particles at the oil-water interface for only two of those froths: DINCH-PVC and heptane-HMDS modified silica. Both of those findings were desirable. The toluene-PS suspected froths were found to be PS aggregates that had adsorbed toluene and creamed at the top of the suspension. This is undesirable and suggests the attractive interactions were too strong between toluene and PS.

Overall, two oils appeared to be successfully selective towards the particles chosen to have primarily one type of attractive interaction between them and an oil, while the other oil also appeared to be selective, but not with the particle chosen to have primarily attractive π - π intermolecular interactions. DINCH was found to be an oil that could potentially be used to selectively remove PVC from a binary particle suspension with either PS or HMDS modified silica, while heptane could potentially be used to selectively remove HMDS modified silica from a binary particle suspension with either PVC or PS. Toluene cannot be used as an oil to selectively remove PS particles from binary particle suspensions via PS adsorption to the oil-water interface because the attractive intermolecular interactions between PS and toluene were too strong. However, toluene could potentially be used to selectively remove PVC from a binary suspension with HMDS modified silica. For the set of three oil and particle combinations tested in this thesis, toluene was not found to be a potential oil that could selectively remove PS particles when the oil and particle have primarily attractive π - π interactions between them. So, the toluene-PS combination is considered to be unsuccessful. Figure 22 on the next page provides a visual

representation of which combinations were found to be successful. Future work will consist of finding an oil and particle combination that interacts primarily through π - π interactions and satisfies the requirements of selectivity. A potential combination could be phenyltrimethoxysilane modified silica and chlorobenzene.

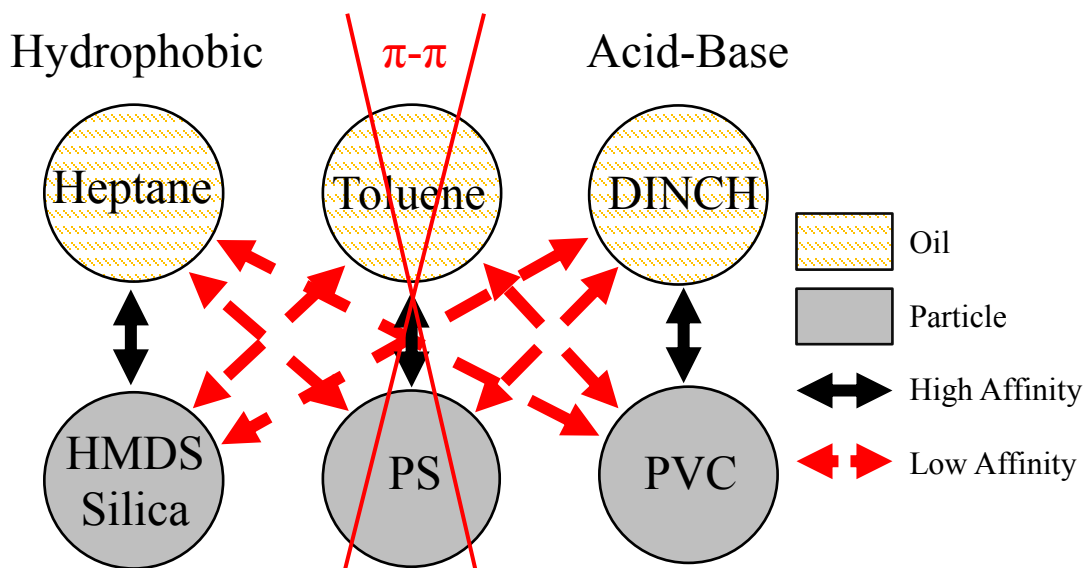


Figure 22. Heptane-HMDS modified silica and DINCH-PVC were found to be successful combinations. The toluene and PS combination was unsuccessful (as shown with the red “x” drawn over the combination).

CHAPTER 3: STRENGTH OF PARTICLE AFFINITY FOR OIL-WATER INTERFACE

3.1 Overview

The goal of this chapter is to quantify the strength of adsorption of the particles to each oil-water interface. The strength of a particle's affinity for an interface was found by investigating the thermodynamics of particle adsorption to the interface. Oil-water interfacial tensions of the pure liquids were measured via pendant drop tensiometry, while the three phase contact angles were determined via the hysteresis method. The mean particle sizes were found by analyzing scanning electron microscopy images and performing dynamic light scattering. Using these measured values allows for the detachment energy to be determined for a particle at an oil-water interface, which would provide a measure of the strength of the particle's affinity for the interface.

3.2 Background and Theory

Standard froth flotation uses air bubbles to introduce an air-water interface to an aqueous solution to which micron-sized particulate contaminants can adsorb to. Some of those contaminant particles may be too hydrophilic to adsorb strongly to the interface, which could cause them to desorb from the interface and return to the aqueous solution⁸. The concept of using oil-coated bubbles allows for the selection of an oil that can lower the energy well the particle falls into when adsorbing to the interface as shown in Figure 23. This means it would be more difficult to remove the particle from the interface; hence, preventing it from returning to the aqueous solution.

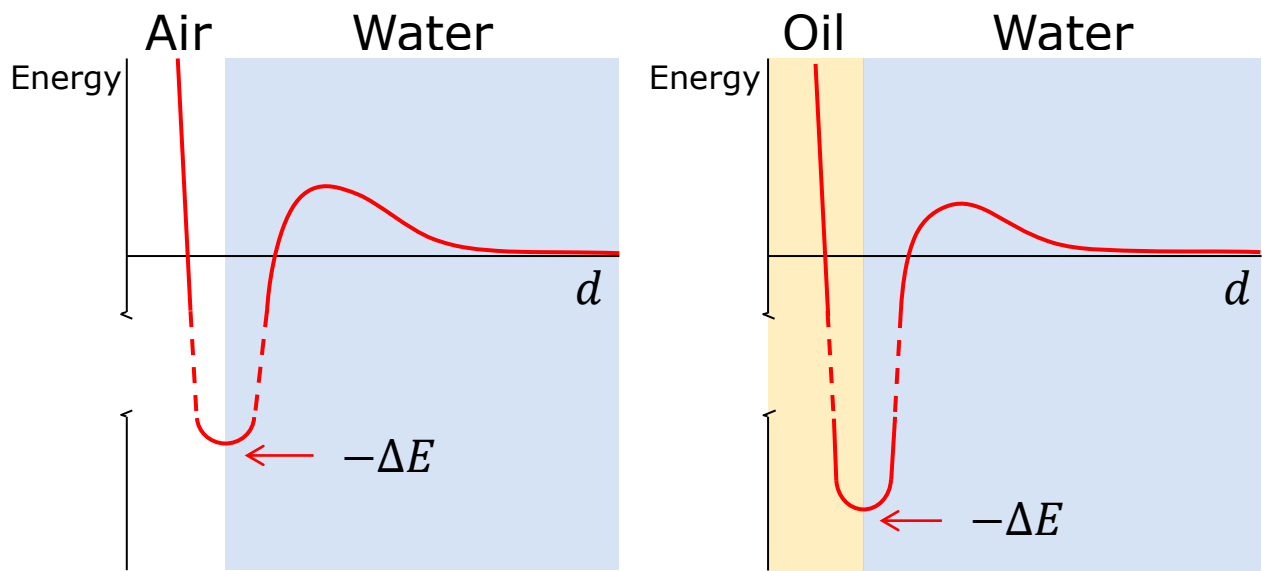


Figure 23. The detachment energy, ΔE , to remove a particle from an interface increases by replacing an air-water interface with an oil-water interface.

This adsorption strength depends on the detachment energy, which (as described in Chapter 2, Section 2.2) is the energy required to remove a particle from an interface. If it is small, then particles will behave like surfactants: adsorbing and de-adsorbing from the interface on a short timescale. If it is very large, then the particles essentially adsorb irreversibly to the interface³⁸. The second scenario is more favorable for removing a targeted particle from an aqueous solution because irreversible adsorption prevents particles from detaching from the oil-coated bubbles and returning to the aqueous solution. Equation 7 is Equation 2 rewritten to show the detachment energy, ΔE , required to remove a particle of radius r from an oil-water interface into the aqueous phase^{38, 43}.

$$\Delta E = \pi r^2 \gamma_{ow} (1 - |\cos \theta|)^2 \quad (7)$$

This equation highlights three factors that influence the detachment energy: the particle size, the oil-water interfacial tension, and the three phase contact angle. Since the particles will be greater than 2 nm in diameter, the particle size will not be a limiting factor in determining whether or not

the particles adsorb irreversibly to the oil-water interface and the most important parameters governing the detachment energy are the contact angle and the oil-water interfacial tension³⁸.

3.3 Methods

3.3.1 Pendant Drop Tensiometry

For quantitative interfacial tension measurements, pendant drop tensiometry was performed with pure oil drops in aqueous solutions using a ramé-hart goniometer/tensiometer. The volume of the drops was kept constant and the interfacial tension was measured via drop shape analysis. The Worthington number, Wo , is a dimensionless number that can be used to gain an understanding of what drop volumes can yield accurate interfacial tension measurements and can be defined as⁶⁸

$$Wo = \frac{V}{V_{max}} \quad (8)$$

where V is the actual drop volume and V_{max} is the theoretical maximum drop volume the interfacial tension force can retain. The closer to one Wo is, the more the interface is allowed to deform without the droplet detaching from the needle and the more accurate the measurements will be.

For heptane drops, the aqueous phase was deionized water. For toluene and DINCH, the aqueous phase was deuterium oxide (heavy water). The heavy water was obtained from Sigma Aldrich and used as received. In addition to the oil-water interfacial tension measurements, the surface tension of de-ionized water and heavy water was measured to be $72.7 \pm 0.6 \text{ mN}\cdot\text{m}^{-1}$ and $73.8 \pm 1.3 \text{ mN}\cdot\text{m}^{-1}$ respectively at $20 \pm 1 \text{ }^\circ\text{C}$. Both of which are within the error of the literature value of $72.75 \pm 0.36 \text{ mN}\cdot\text{m}^{-1}$ at the same temperature⁶⁸⁻⁶⁹. This suggests using heavy water in

place of de-ionized water should have no significant effect on the measured oil-water interfacial tension values.

3.3.2 *Three Phase Contact Angle*

Where a particle is located at an oil-water interface is indicative of how strongly a particle prefers to be at the interface. The angle made between a particle and the oil-water interface provides the information for where the particle is located at the interface. This angle, which is known as three phase contact angle, was measured for all of the possible oil and particle combinations using the hysteresis method. The hysteresis method averages advancing and receding contact angles to obtain an apparent equilibrium contact angle for an inverted sessile drop of oil on the flat surface of a solid pellet mimicking the particles and completely surrounded by water. The main drawback with this method is the pellet surface roughness differs from the surface roughness of particles because of the limitations to eliminating gaps between particles⁷⁰⁻⁷¹ and changes to the particle surfaces when compression forces are applied during the making of the pellets, which can drastically alter the equilibrium contact angle⁷². Despite this problem, this method is still better than another more frequently used method: the static contact angle method. The static contact angle method measures the contact angle of a drop on a flat surface once the system has reached equilibrium. In addition to the drawback that such a surface cannot be made to replicate the surface roughness of the surface of a particle, this method requires the droplet to be small enough that gravitational effects can be ignored⁷³ and assumes the droplet will eventually reach an equilibrium state, which is not always true due to phenomena such as pinning of the liquid-liquid interface due to surface heterogeneity⁷⁴⁻⁷⁵. These additional drawbacks are addressed by using the hysteresis method because there are no limitations on the droplet size (only requirement is that the droplet is axisymmetric)⁷³ and slow movement of the contact line caused

by the drop expanding or contracting overcomes the non-equilibrium pinning states static droplets can experience⁷⁴.

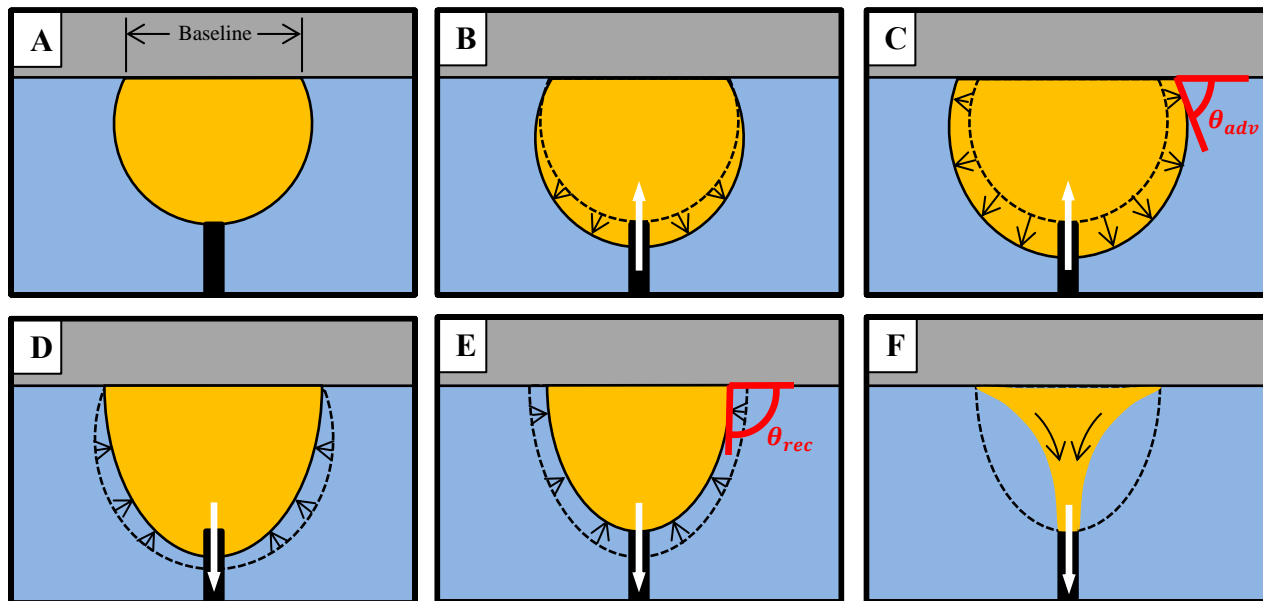


Figure 24. Step-by-step pictures of the hysteresis method with an inverted sessile drop of oil. (A) A 2 μL droplet is deposited on the solid surface and the baseline is recorded. (B) The drop is grown at a rate of 0.125 $\mu\text{L/s}$ and the contact angle changes. (C) When the contact angle equals θ_{adv} , the baseline increases. (D) The droplet is then retracted at a rate of 0.125 $\mu\text{L/s}$ and the contact angle changes again. (E) Once the contact angle equals θ_{rec} , the baseline changes again. (F) Continuing retraction of the droplet will cause the droplet to become distorted and no more meaningful information can be extracted.

A ramé-hart goniometer/tensiometer was used to take images of inverted sessile drops on solid pellet surfaces in aqueous solutions. The images were analyzed via drop shape analysis to record the baseline and contact angle. Figure 24 shows the steps that were followed to obtain the advancing and receding contact angles. Initially, a 2 μL droplet of oil was dispensed on a solid pellet surface submerged in water and the baseline was noted (Figure 24A). Next, the drop was grown at a rate of 0.125 $\mu\text{L/s}$ until the baseline increases, which is when the advancing contact angle, θ_{adv} , was recorded (Figure 24B and Figure 24C). Then, the oil in the droplet was removed through the syringe needle until the droplet baseline changed, which is when the receding contact

angle, θ_{rec} , was recorded (Figure 24D and Figure 24E). Further removal of oil results in the droplet width approaching the dimension of the syringe needle, which is when the contact angle rapidly approaches zero (Figure 24F).

To determine the apparent equilibrium contact angle, θ_{avg} , the advancing and receding contact angles can be averaged using either one of the two following equations⁷⁶⁻⁷⁷:

$$\theta_{avg} = \frac{\theta_{adv} + \theta_{rec}}{2} \quad (9)$$

$$\cos(\theta_{avg}) = \frac{\cos(\theta_{adv}) + \cos(\theta_{rec})}{2} \quad (10)$$

Since Equations 9 and 10 usually yield very similar results⁷⁸ and Equation 9 requires fewer mathematical steps to be taken to find the apparent equilibrium contact angle, Equation 9 was used when determining the apparent equilibrium contact angle.

3.3.3 Particle Size

To obtain an accurate estimate of the strength of particle adsorption to an oil-water interface, is desirable to be able to know the average size of the particles in an aqueous solution. Dynamic light scattering (DLS) makes this possible by measuring the fluctuations in the scattered light intensity due to the Brownian motion of particles and calculating a hydrodynamic diameter using data from these measurements and the Stokes-Einstein equation⁷⁹. But, this technique has some limitations. For example, the larger in size a particle is, the lower the maximum total number of particles can be dispersed in the solution and not experience effects due to particle interactions⁸⁰. This results in a smaller sample set being used to determine the particle size distribution and increases the error⁸¹. Also, the particle size and weight matter because Brownian forces must

dominate the gravitational forces; otherwise, particles can undergo noticeable sedimentation or creaming motion, which effect the DLS measurements. For this reason, DLS usually is only feasible for particles less than a few microns in size⁸⁰. HMDS modified silica were expected to have particle sizes in the nanometer range, so DLS was performed on them in water using a Malvern Zetasizer Nanoseries ZS90. For PVC and PS, which are expected to have average particle diameters around 30 μm (according to Zhang et al.²⁴) and 8 μm (according to the manufacturer's specifications sheet) respectively, their particle size distributions and average diameters determined by using ImageJ to analyze scanning electron microscopy (SEM). SEM images were obtained for the PVC and PS particles using a Hitachi SU8010 SEM with a 5 keV beam. The particle diameters for PVC and PS were measured to the nearest 5 μm and 2 μm respectively. A typical SEM image of PVC and PS are shown in Figure 25 and Figure 26 respectively.

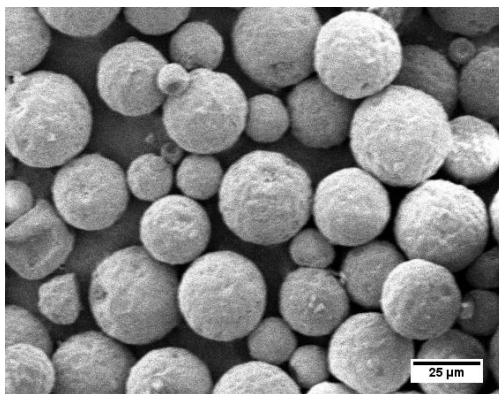


Figure 25. Typical SEM image of washed PVC particles.

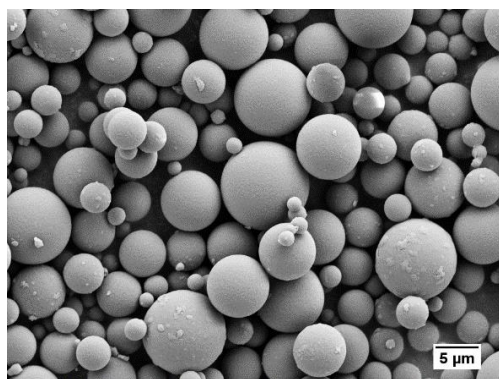


Figure 26. Typical SEM image of washed PS particles.

The average particle diameter was a number-average diameter, d_n , calculated using data from the particle size distributions and⁸²

$$d_n = \sum_i x_i d_i \quad (11)$$

where x_i is the number fraction of particles in the i^{th} interval characterized by a middle size diameter, d_i . The number fraction was found using⁸²

$$x_i = \frac{n_i}{\sum_i n_i} \quad (12)$$

where n_i is the number of particles in the i^{th} interval.

3.4 Results

3.4.1 Pendant Drop Tensiometry

Table 1 lists the measured and literature oil-water interfacial tension values for each of the three oils. The tension values remained relatively constant over the entire duration of the measurements as shown in Figure 27, Figure 28, and Figure 29. To the author's knowledge, the DINCH-water interfacial tension is the first time its interfacial tension with water has been recorded. The heptane and the toluene interfacial tensions with water were 3.7% and 3.5% lower than their literature values respectively. This could be the result of not purifying the oils enough, as the oils in this study were purified with the equivalent of one pass through a silica gel column. Zeppieri et al distilled heptane and passed it multiple times through an alumina column to obtain the heptane-water interfacial tension value of 51.24 ± 0.04 mN/m⁸³. Following this method would not only remove surface active agents, but the distillation would remove branched heptane isomers, which can lower the heptane-water interfacial tension⁸⁴. For more accurate measurements in the

future, the oils in this study should undergo more passes through either silica gel or aluminum oxide columns to insure complete removal of surface active components. In conclusion, the oils used in this study still had impurities when used, but with their interfacial tensions only deviating about 3.5% from their literature values, this is expected to cause the calculated particle affinity for the oil-water interface to be approximately 3.5% less than the actual values would be with a pure oil phase.

Table 1. Experimental and literature oil-water interfacial tension values along with the temperature.

Oil	Experimental γ_{ow} (mN·m ⁻¹)	Literature γ_{ow} (mN·m ⁻¹)	Temperature (°C)
Heptane	49.3 ± 0.7	51.2 ^{a, b}	20 ± 1
Toluene	35.8 ± 0.3	37.1 ± 0.1 ^c	20 ± 1
DINCH	31.5 ± 0.2	N/A	23.2 ± 0.2

^a = Aveyard and Haydon⁸⁵

^b = Zeppieri et al.⁸³

^c = Saien and Akbari⁸⁶

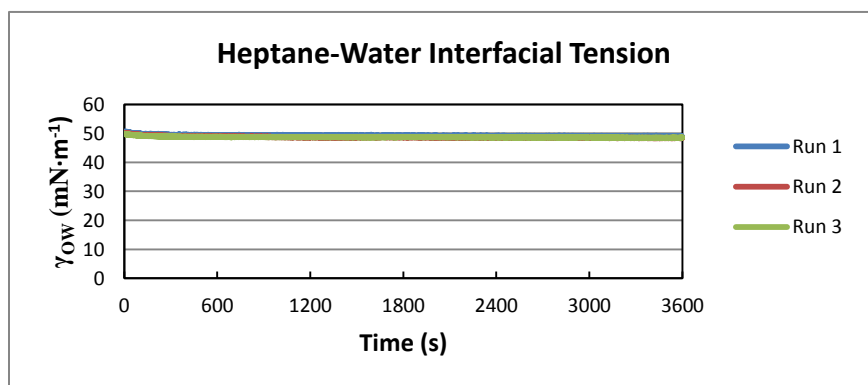


Figure 27. Interfacial tension measurements of a pendant drop of heptane in deionized water.

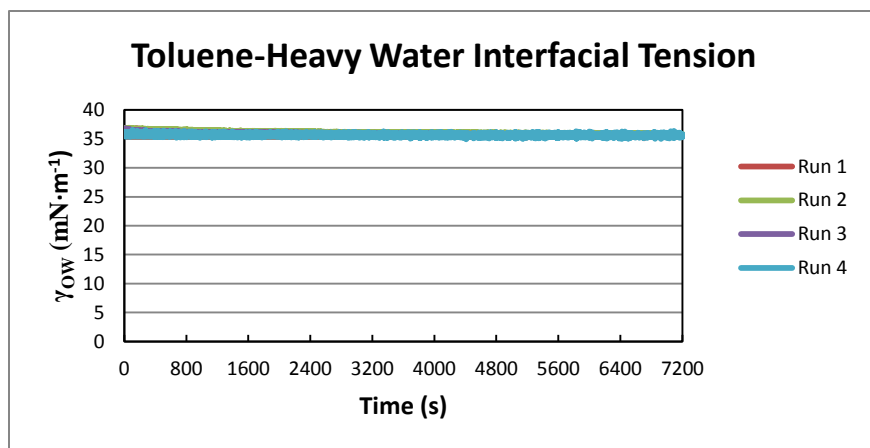


Figure 28. Interfacial tension measurements of a pendant drop of toluene in heavy water.

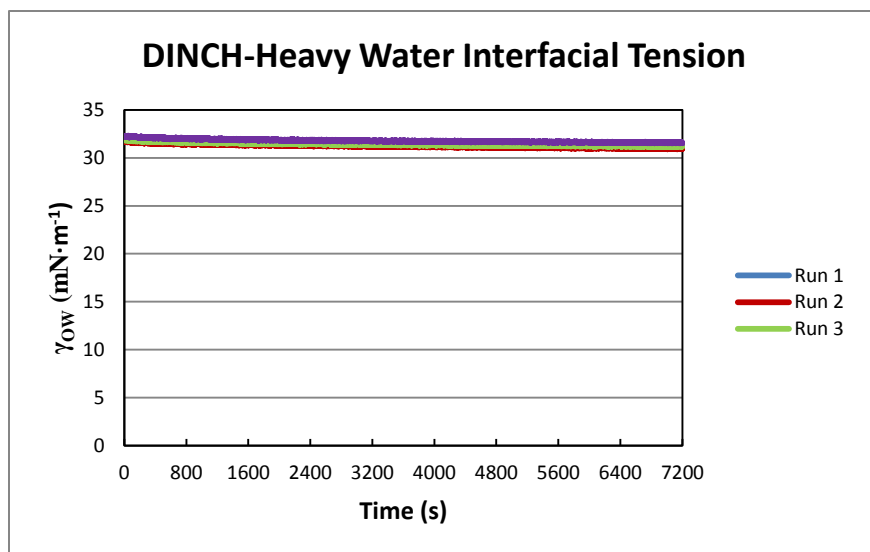


Figure 29. Interfacial tension measurements of a pendant drop of diisononyl cyclohexanedicarboxylate in heavy water.

3.4.2 Three Phase Contact Angle

Figure 30 shows the three phase contact angles through the aqueous phase for the particles for which it was possible to obtain the angles via the hysteresis method. Table 2 displays the numerical values of these contact angles.

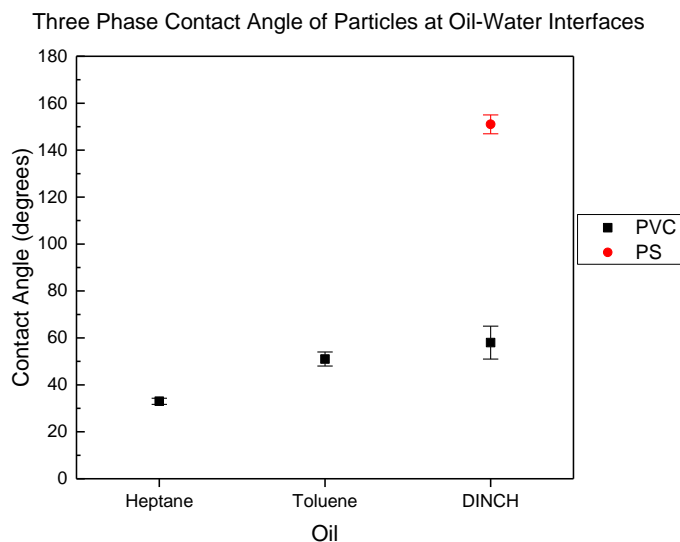


Figure 30. Three phase contact angle as measured through the aqueous phase via the hysteresis method.

Table 2. Numerical values of the contact angles displayed in Figure 30.

	Heptane	Toluene	DINCH
PVC	33.0° ± 1.3°	51° ± 3°	58° ± 7°
PS	Oil wicked by pellet	Oil wicked by pellet	151° ± 4°
HMDS Silica	Oil wicked by pellet	Oil wicked by pellet	Oil wicked by pellet

The measured contact angles of the heptane-water-PVC system were in a range that suggested the particle would be mostly wetted by water at the interface and not wetted enough by the oil for strong adsorption to the interface to occur. This observation is consistent with the prior observation that foams produced with heptane and PVC had both poor foaming ability and poor foam stability. The DINCH-water-PS system also had a contact angle far above 90°, that the oil

would mostly wet the particle and lead to a weak particle affinity for the DINCH-water interface. This is consistent with the observation that a foam could not be created with DINCH and PS.

The angles for a PVC particle at the toluene-water and DINCH-water interfaces are within the region where particles can stabilize these foams. Zhang et al. suggest that particles with angles in this range (45° - 60°) should create semi-stable foams²⁴. In contrast, both the toluene-water-PVC and DINCH-water-PVC systems in this work produced large foam heads that remained almost wholly intact after one month. So, while both foams are stable, PVC appears to have a higher affinity for the DINCH-water interface than for the toluene-water interface, as evidenced by a contact angle that is closer to 90° at the DINCH-water interface.

For HMDS modified silica and some of the PS pellets, the contact angle could not be determined because the pellets wicked the oil droplet. If the hysteresis method is to be used to determine the contact angles, then other methods of producing a solid surface to mimic the surfaces of the particles will be required. Examples of such methods include modifying clean glass slides with HMDS to represent the surfaces of HMDS silica particles and casting a thin polystyrene film onto a glass substrate to mimic the surfaces of PS particles.

3.4.3 Average Particle Sizes

Figure 31 and Figure 32 show typical particle size distributions for the PVC and PS particles, while Table 3 shows the average particle diameter and radius for each type of particle.

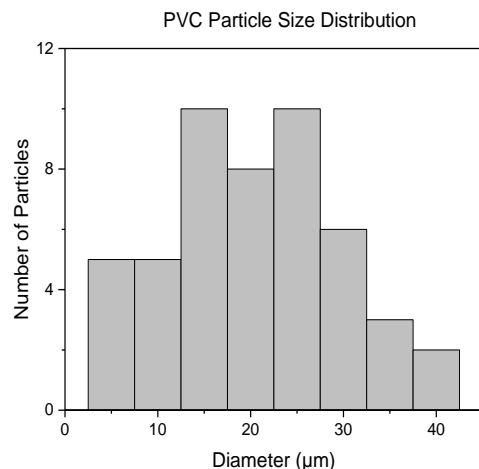


Figure 31. Typical particle size distribution of PVC particles.

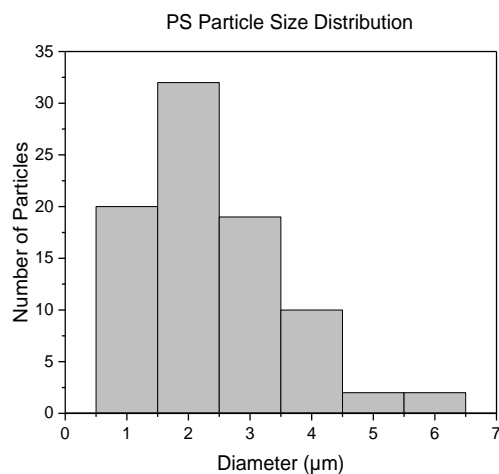


Figure 32. Typical particle size distribution of PS particles.

The average particle sizes for PVC and PS were less than their expected values of 29.6 μm and 8 μm respectively. The size distributions for PVC were all very broad, so it is possible that the average diameter varied from that found by Zhang et al.²⁴ due to either minor differences in the batches of particles obtained from the manufacturer or a small sample set. The PS particle size was smaller than expected, which suggests that the larger particles may have been lost in the pretreatment steps. As expected, the HMDS modified silica particles were much larger than the particle size listed by the manufacturer (7 nm), which means these particles form aggregates. On

the basis of these particle sizes alone, the magnitude of the affinity a particle has for an oil-water interface will be greater for PVC than for PS, which will be greater than for HMDS modified silica.

Table 3. Average particle sizes.

Particle	Diameter (μm)
PVC	21 ± 2
PS	2.1 ± 0.2
HMDS modified Silica	0.093 ± 0.003

3.4.4 Particle Affinity for Oil-Water Interface

Figure 33 shows the calculated adsorption strength PVC and PS particles have for oil-water interfaces. The energies were calculated using Equation 7, the measured interfacial tensions, three phase contact angles, and particle radii.

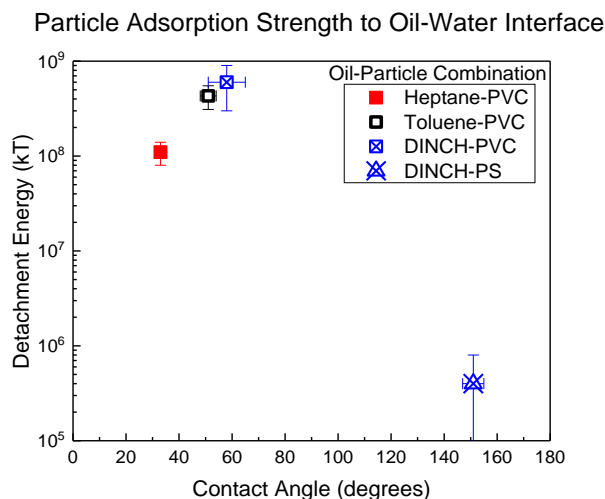


Figure 33. PVC and PS particle adsorption strength to oil-water interfaces in units of $k_B T$.

From this graph, it is evident that the particles that adsorb the strongest to an interface (PVC to toluene-water and PVC to DINCH-water) are also those that created stable capillary foams in Chapter 2. Also, the graph suggests PVC has a lower affinity for the heptane ($1.12 \times 10^8 k_B T$) and further supports the results seen in the foaming ability (Chapter 2, Section 2.5.1) and foam stability (Chapter 2, Section 2.5.2) sections, as the PVC and heptane system formed a part foam and part capillary suspension. Meanwhile, PS had an even lower affinity for the DINCH-water interface ($4.32 \times 10^5 k_B T$), which also agrees with earlier tests when foams were not observed for the DINCH and PS system. As mentioned in Section 3.4.1, these calculated values are likely to be approximately 3.5% less than they would be with pure oil phases, but this does not have a significant effect on the observed trends in the data. So, these results confirm that PVC particles strongly adsorb to both the toluene-water and DINCH-water interfaces. They also show that PVC and PS have a low affinity for the heptane-water and DINCH-water interfaces respectively.

3.5 Concluding Remarks

The goal of this Chapter was to quantify the strength of affinity particles have to each possible oil-water interface. To do this, three quantities were measured: the oil-water interfacial tension, the three phase contact angle, and the particle radius. Oil-water interfacial tensions were measured using pendant drop tensiometry. The three phase contact angles were determined using the hysteresis method. While the particle radii were measured using DLS for nanometer-sized particles and analyzing SEM images for the micron-sized particles.

The results of the oil-water interfacial measurements suggest that the oils were impure, but the measured interfacial tension values did not seem to differ significantly enough from the

literature values for them to significantly affect the calculated affinity a particle has for oil-water interfaces. The DINCH-water interfacial tension was measured for the first time and, in order to insure this value is accurate, future tests will need to be done with DINCH that has undergone multiple passes through a silica gel column to ensure it is pure. The measured particle sizes suggest that, based off of particle size, the magnitude of the strength of particle adsorption to an oil-water interface will rank in the following order: PVC > PS > HMDS modified silica. The contact angles could only be measured for 4 of the 9 possible oil and particle combinations as the oil was wicked by the solid pellets representing the surfaces of PS and HMDS modified silica particles for 5 of the combinations. Possible solutions to these problems are to use a HMDS modified glass slide and a thin polystyrene film on a glass substrate to represent HMDS modified silica particles and PS particles respectively.

While these methods could provide solid surfaces for which contact angle measurements can be made for the attempts were the oil droplets were wicked by the pellets, these flat surfaces could vary from the actual particle surfaces in surface roughness and surface chemistry. The modified glass slides could differ in surface roughness and the packing arrangement of HMDS adsorbed to the surface could vary from the surface roughness and the packing arrangement of the HMDS on the silica nanoparticle surfaces⁸⁷⁻⁸⁸, while the surface roughness of thin polystyrene films will change depending on the solvent used in their production⁸⁹. Since differences in surface roughness can drastically affect the contact angle⁷², a better method should be used to measure the contact angles of particles at oil-water interfaces. One such method is the gel-trapping technique, which involves spreading colloidal particles at an interface and gelling the aqueous phase with a non-surface-active gelling agent to trap the particles⁷⁰. The top phase is then removed and replaced with curable polydimethylsiloxane (PDMS). The PDMS would be cured, peeled off the gel, and

imaged using a SEM. Future work will use the gel-trapping technique to measure the contact angles of particles at oil-water interfaces.

Using Equation 7 and the results from the pendant drop tensiometry, contact angle, and particle size measurements, the affinity of PVC and PS particles to oil-water interfaces was calculated. The results confirmed that PVC does have a high affinity for the DINCH-water interface and the toluene-water interface, while it has a low affinity for the heptane-water interface. Also, PS was shown to have a low affinity for the DINCH-water interface. Future work will involve quantifying the acidity and basicity of both the PVC particles and DINCH in order to prove acid-base interactions occur between DINCH and PVC. The method to determine the acidity and basicity of the liquid DINCH will roughly follow that outlined by Lee et al.⁹⁰, while the method to determine the acidity and basicity of the solid PVC will follow that described by Van Oss et al⁹¹. Completing the future work would provide a method for tuning the selectivity of oil-water interfaces and prove the DINCH and PVC combination is a good combination for an oil and particle that have primarily acid-base interactions between them.

CHAPTER 4: CONCLUSIONS AND RECOMMENDATIONS

Many applications require the selective removal of particulate contaminants from aqueous solutions. Standard froth flotation is a very efficient process that is commonly used in these applications to indiscriminately remove very hydrophobic micron-sized particulate contaminants. It is preferable to have a method that can take advantage of the efficiency of such a process and be selective with regards to what particles are to be removed from the solution.

Coating the air bubbles with a thin layer of oil allows for the possibility of selecting oils that have sufficiently strong attractive intermolecular interactions with a targeted particle, and correspondingly weak attractive interactions with other particles in the suspension, so as to achieve preferential wetting at the oil-water interface. This would cause only the targeted particle to strongly adsorb to the oil-water interface and rise to the top of the solution with the bubble, while the other particles remain in the solution. Demonstrating this concept of using oil-coated air bubbles to selectively remove particulate contaminants from process effluents, called “affinity flotation,” would be novel. This study focuses on the first step required to prove affinity flotation, which is examining potential oil and particle combinations that could be used to demonstrate the idea of affinity flotation.

The main goals of this study are to (1) find three oils that can selectively remove only one particle from an aqueous suspension via one of the following attractive intermolecular interactions: hydrophobic, π - π , and acid-base; and (2) quantify the strength of the affinity the particles have for each of the possible oil-water interfaces. Potential oil and particle combinations were chosen based off the propensity of their molecular structures to have one of the aforementioned intermolecular interactions between them. These potential combinations were then screened using simple foaming

ability and foam stability tests. Confocal microscopy was used to verify any froths that could not be easily verified through the foaming ability and foam stability tests. The results of these tests suggest the oils are all selective to one type of particle; however, toluene was not selective to the particle chosen for its propensity to have primarily attractive π - π interactions with it, which was PS. The other two oils, DINCH and heptane, were found to be selective for the particles (PVC and HMDS modified silica respectively) chosen to have primarily acid-base and hydrophobic interactions with their respective oil. So, DINCH-PVC and heptane-HMDS modified silica appeared to be successful oil and particle combinations, while toluene-PS was not. Future work will consist of finding an oil and particle combination that interacts primarily through π - π interactions and satisfies the requirements of selectivity. A potential combination could be phenyltrimethoxysilane modified silica and chlorobenzene.

To accomplish the second main goal of this study, three quantities were measured: the oil-water interfacial tension, the three phase contact angle, and the particle radius. Oil-water interfacial tensions were measured using pendant drop tensiometry. The three phase contact angles were determined using the hysteresis method, and the particle radii were measured using DLS for nanometer-sized particles and analyzing SEM images for the micron-sized particles.

The results of the oil-water interfacial measurements suggest that the oils were impure, but the measured interfacial tension values did not seem to differ significantly enough from the literature values for them to significantly affect the calculated affinity a particle has for oil-water interfaces. The DINCH-water interfacial tension was measured for the first time. Future tests will be done with DINCH that has undergone multiple passes through a silica gel column to insure it is pure and the measured value is accurate. The contact angles could only be measured for 4 of the 9 possible oil and particle combinations as the oil was wicked by the solid pellets representing the

surfaces of PS and HMDS modified silica particles for 5 of the combinations. Because of this and the additional problem that the surface roughness of the particles is not easy to represent using coated substrates, the method for measuring contact angles is recommended to be the gel-trapping technique in future work. The results of the particle size measurements suggest that the magnitude of the affinity a particle has for an oil-water interface will be greater for PVC than for PS, which will be greater than for HMDS modified silica.

Using Equation 7 and the results from the pendant drop tensiometry, contact angle, and particle size measurements, the affinity of PVC and PS particles to oil-water interfaces was calculated. The results confirmed that PVC does have a high affinity for the DINCH-water interface, while it has a low, but still somewhat high, affinity for the toluene-water interface and a low affinity for the heptane-water interface. Also, PS was shown to have a low affinity for the DINCH-water interface. Future work will be done to quantify the acidity and basicity of both the PVC particles and DINCH in order to prove acid-base interactions are taking place between DINCH and PVC. This would prove that the DINCH and PVC combination is a good combination for an oil and particle that have primarily acid-base interactions between them.

APPENDIX A: MISCELLANEOUS FIGURES

Confocal microscopy images of heptane-HMDS modified silica foams are shown in Figure 34, Figure 35, and Figure 36.

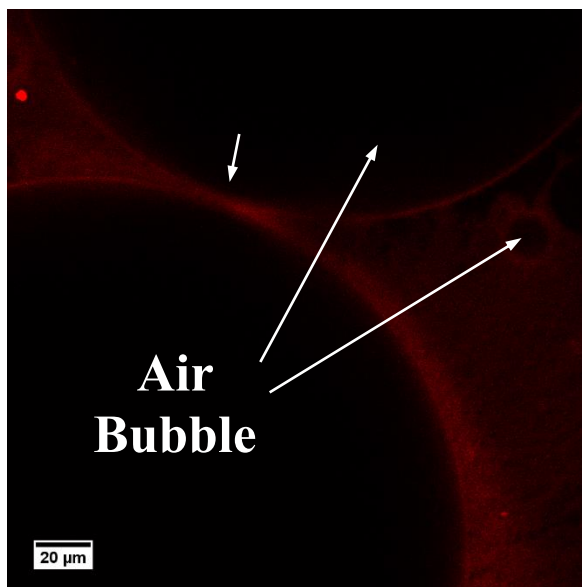


Figure 34. Coalescence being temporarily arrested by the HMDS modified silica particle stabilized heptane-water interface of two large bubbles.

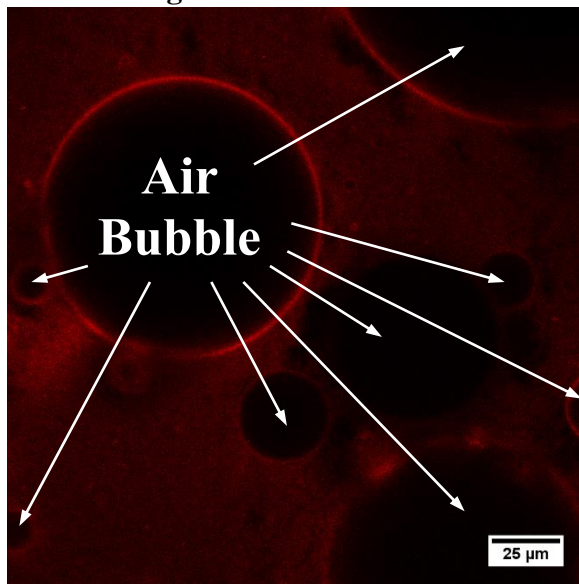


Figure 35. Multiple air bubbles stabilized by HMDS modified silica particles at the heptane-water interface around the bubbles.

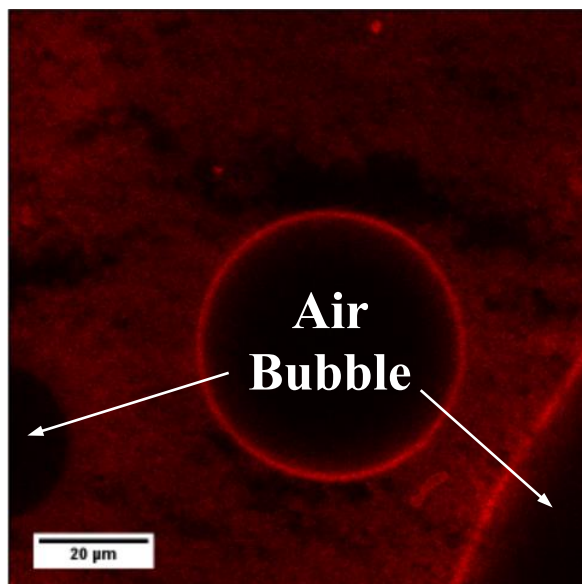


Figure 36. HMDS modified silica particles stabilizing the heptane-water interface coating an air bubble.

REFERENCES

1. Guo, J.; Filpponen, I.; Johansson, L.-S.; Mohammadi, P.; Latikka, M.; Linder, M. B.; Ras, R. H. A.; Rojas, O. J., Complexes of Magnetic Nanoparticles with Cellulose Nanocrystals as Regenerable, Highly Efficient, and Selective Platform for Protein Separation. *Biomacromolecules* **2017**, *18* (3), 898-905.
2. Keiblinger, K. M.; Fuchs, S.; Zechmeister-Boltenstern, S.; Riedel, K., Soil and leaf litter metaproteomics—a brief guideline from sampling to understanding. *FEMS Microbiology Ecology* **2016**, *92* (11).
3. Preece, K. E.; Hooshyar, N.; Krijgsman, A. J.; Fryer, P. J.; Zuidam, N. J., Intensification of protein extraction from soybean processing materials using hydrodynamic cavitation. *Innovative Food Science & Emerging Technologies* **2017**, *41* (Supplement C), 47-55.
4. Rubio, J.; Souza, M. L.; Smith, R. W., Overview of flotation as a wastewater treatment technique. *Minerals Engineering* **2002**, *15* (3), 139-155.
5. Shammass, N. K.; Bennett, G. F., Principles of Air Flotation Technology. In *Handbook of Environmental Engineering, Volume 12: Flotation Technology*, Wang, L. K. e. a., Ed. Springer Science + Business Media, LLC: New York, NY, 2010; Vol. 12, pp 1-47.
6. Voronin, N. N.; Dibrov, I. A., *Classification of Flotation Processes in Wastewater Decontamination*. 1998; Vol. 124.
7. Rodrigues, R. T.; Rubio, J., DAF—dissolved air flotation: Potential applications in the mining and mineral processing industry. *International Journal of Mineral Processing* **2007**, *82* (1), 1-13.
8. Rao, S. R., *Surface Chemistry of Froth Flotation Volume 1: Fundamentals*. Second ed.; Kluwer Academic Publishers/Plenum Publishers: New York, NY, 2004; Vol. 1.
9. Araujo, A. C.; Viana, P. R. M.; Peres, A. E. C., Reagents in iron ores flotation. *Minerals Engineering* **2005**, *18* (2), 219-224.
10. Zhao, Y.; Deng, Y.; Zhu, J. Y., *Roles of surfactants in flotation deinking*. 2004; Vol. 14.
11. Gübitz, G. M.; Mansfield, S. D.; Böhm, D.; Saddler, J. N., Effect of endoglucanases and hemicellulases in magnetic and flotation deinking of xerographic and laser-printed papers. *Journal of Biotechnology* **1998**, *65* (2), 209-215.
12. Bradshaw, D. J. Synergistic Effects Between Thiol Collectors Used in the Flotation of Pyrite. University of Cape Town, University of Cape Town, 1997.
13. Von Rybinski, W.; Schwuger, M. J., Adsorption of surfactant mixtures in froth flotation. *Langmuir* **1986**, *2* (5), 639-643.

14. Coetzer, G.; Davidtz, J. C., Sulphydryl collectors in bulk and selective flotation. Part 2. Covalent dithiocarbamate derivatives. *Journal of the Southern African Institute of Mining and Metallurgy* **1989**, 89 (11).
15. Hanumantha Rao, K.; Forssberg, K. S. E., Mixed collector systems in flotation. *International Journal of Mineral Processing* **1997**, 51 (1), 67-79.
16. Lotter, N. O.; Bradshaw, D. J., The formulation and use of mixed collectors in sulphide flotation. *Minerals Engineering* **2010**, 23 (11), 945-951.
17. Su, L.; Xu, Z.; Masliyah, J., Role of oily bubbles in enhancing bitumen flotation. *Minerals Engineering* **2006**, 19 (6), 641-650.
18. Wallwork, V.; Xu, Z.; Masliyah, J., Bitumen Recovery with Oily Air Bubbles. *The Canadian Journal of Chemical Engineering* **2003**, 81 (5), 993-997.
19. Tarkan, H. M.; Finch, J. A., Air-assisted solvent extraction: towards a novel extraction process. *Minerals Engineering* **2005**, 18 (1), 83-88.
20. Chen, F.; Finch, J. A.; Distin, P. A.; Gomez, C. O., AIR ASSISTED SOLVENT EXTRACTION. *Canadian Metallurgical Quarterly* **2003**, 42 (3), 277-280.
21. Gomez, C.; Acuna, C.; Finch, J. A.; Pelton, R., Aerosol-enhanced flotation deinking of recycled paper. *Pulp and Paper Canada* **2001**, 102 (10), 28-30.
22. Polat, M.; Polat, H.; Chander, S., Physical and chemical interactions in coal flotation. *International Journal of Mineral Processing* **2003**, 72 (1), 199-213.
23. Taggart, A. F., *Handbook of Ore Dressing*. John Wiley & Sons: 1927; p 1679.
24. Zhang, Y.; Wu, J.; Wang, H.; Meredith, J. C.; Behrens, S. H., Stabilization of Liquid Foams through the Synergistic Action of Particles and an Immiscible Liquid. *Angewandte Chemie* **2014**, 126 (49), 13603-13607.
25. Zhang, Y.; Allen, M. C.; Zhao, R.; Deheyn, D. D.; Behrens, S. H.; Meredith, J. C., Capillary Foams: Stabilization and Functionalization of Porous Liquids and Solids. *Langmuir* **2015**, 31 (9), 2669-2676.
26. Zhang, Y.; Shitta, A.; Meredith, J. C.; Behrens, S. H., Bubble Meets Droplet: Particle-Assisted Reconfiguration of Wetting Morphologies in Colloidal Multiphase Systems. *Small* **2016**, 12 (32), 4307-4307.
27. Zhang, Y.; Wang, S.; Zhou, J.; Zhao, R.; Benz, G.; Tcheimou, S.; Meredith, J. C.; Behrens, S. H., Interfacial Activity of Nonamphiphilic Particles in Fluid–Fluid Interfaces. *Langmuir* **2017**, 33 (18), 4511-4519.

28. Zhang, Y.; Wang, S.; Zhou, J.; Benz, G.; Tcheimou, S.; Zhao, R.; Behrens, S. H.; Meredith, J. C., Capillary Foams: Formation Stages and Effects of System Parameters. *Industrial & Engineering Chemistry Research* **2017**, *56* (34), 9533-9540.
29. Wang, S. Z., Y.; Meredith, J.C.; Behrens, S.H.; Tripathi, M.K.; Sahu, K.C., The dynamics of rising oil-coated bubbles: experiments and simulations. **2017**.
30. Venkataraman, P.; Sunkara, B.; St. Dennis, J. E.; He, J.; John, V. T.; Bose, A., Water-in-Trichloroethylene Emulsions Stabilized by Uniform Carbon Microspheres. *Langmuir* **2012**, *28* (2), 1058-1063.
31. Kaiser, A.; Liu, T.; Richtering, W.; Schmidt, A. M., Magnetic Capsules and Pickering Emulsions Stabilized by Core-Shell Particles. *Langmuir* **2009**, *25* (13), 7335-7341.
32. Saleh, N.; Sarbu, T.; Sirk, K.; Lowry, G. V.; Matyjaszewski, K.; Tilton, R. D., Oil-in-Water Emulsions Stabilized by Highly Charged Polyelectrolyte-Grafted Silica Nanoparticles. *Langmuir* **2005**, *21* (22), 9873-9878.
33. Jansen, F.; Harting, J., From bijels to Pickering emulsions: A lattice Boltzmann study. *Physical Review E* **2011**, *83* (4), 046707.
34. Tavecchi, J. W.; Thijssen, J. H. J.; Schofield, A. B.; Clegg, P. S., Novel, Robust, and Versatile Bijels of Nitromethane, Ethanediol, and Colloidal Silica: Capsules, Sub-Ten-Micrometer Domains, and Mechanical Properties. *Advanced Functional Materials* **2011**, *21* (11), 2020-2027.
35. Cates, M. E.; Clegg, P. S., Bijels: a new class of soft materials. *Soft Matter* **2008**, *4* (11), 2132-2138.
36. Frijters, S.; Günther, F.; Harting, J., Domain and droplet sizes in emulsions stabilized by colloidal particles. *Physical Review E* **2014**, *90* (4), 042307.
37. Johnson, K. L.; Kendall, K.; Roberts, A. D., Surface energy and the contact of elastic solids. *Proceedings of the Royal Society of London. A. Mathematical and Physical Sciences* **1971**, *324* (1558), 301.
38. Aveyard, R.; Binks, B. P.; Clint, J. H., Emulsions stabilised solely by colloidal particles. *Advances in Colloid and Interface Science* **2003**, *100-102* (Supplement C), 503-546.
39. Ramsden, W., Separation of solids in the surface-layers of solutions and 'suspensions' (observations on surface-membranes, bubbles, emulsions, and mechanical coagulation).—Preliminary account. *Proceedings of the Royal Society of London* **1904**, *72* (477-486), 156-164.
40. Pickering, S. U., CXCVI.-Emulsions. *Journal of the Chemical Society, Transactions* **1907**, *91* (0), 2001-2021.
41. Jin, H.; Zhou, W.; Cao, J.; Stoyanov, S. D.; Blijdenstein, T. B. J.; de Groot, P. W. N.; Arnaudov, L. N.; Pelan, E. G., Super stable foams stabilized by colloidal ethyl cellulose particles. *Soft Matter* **2012**, *8* (7), 2194-2205.

42. Binks, B. P., Particles as surfactants—similarities and differences. *Current Opinion in Colloid & Interface Science* **2002**, 7 (1), 21-41.
43. Hunter, T. N.; Pugh, R. J.; Franks, G. V.; Jameson, G. J., The role of particles in stabilising foams and emulsions. *Advances in Colloid and Interface Science* **2008**, 137 (2), 57-81.
44. Hildebrand, J. H., A Critique of the Theory of Solubility of Non-Electrolytes. *Chemical Reviews* **1949**, 44 (1), 37-45.
45. Hansen, C. M., The Universality of the Solubility Parameter. *Product R&D* **1969**, 8 (1), 2-11.
46. Barton, A. F. M., Solubility parameters. *Chemical Reviews* **1975**, 75 (6), 731-753.
47. Peiffer, D. G., The molecular factors affecting the solubility parameter. *Journal of Applied Polymer Science* **1980**, 25 (3), 369-380.
48. Stefanis, E.; Panayiotou, C., Prediction of Hansen Solubility Parameters with a New Group-Contribution Method. *International Journal of Thermophysics* **2008**, 29 (2), 568-585.
49. Beerbower, A.; Hill, M. W., *McCutcheon's Detergents and Emulsifiers Annual*. Allured Publ. Co.: Ridgewood, NJ, 1971.
50. Holtzscherer, C.; Candau, F., Application of the cohesive energy ratio concept (CER) to the formation of polymerizable microemulsions. *Colloids and Surfaces* **1988**, 29 (4), 411-423.
51. Salager, J.-L.; Forgiarini, A. M.; Bullón, J., How to Attain Ultralow Interfacial Tension and Three-Phase Behavior with Surfactant Formulation for Enhanced Oil Recovery: A Review. Part 1. Optimum Formulation for Simple Surfactant–Oil–Water Ternary Systems. *Journal of Surfactants and Detergents* **2013**, 16 (4), 449-472.
52. Candau, F.; Pabon, M.; Anquetil, J.-Y., Polymerizable microemulsions: some criteria to achieve an optimal formulation. *Colloids and Surfaces A: Physicochemical and Engineering Aspects* **1999**, 153 (1), 47-59.
53. Buchert, P.; Candau, F., Polymerization in microemulsions: I. Formulation and structural properties of microemulsions containing a cationic monomer. *Journal of Colloid and Interface Science* **1990**, 136 (2), 527-540.
54. Hunter, C. A.; Sanders, J. K. M., The nature of .pi.-.pi. interactions. *Journal of the American Chemical Society* **1990**, 112 (14), 5525-5534.
55. Fowkes, F. M.; Mostafa, M. A., Acid-Base Interactions in Polymer Adsorption. *Industrial & Engineering Chemistry Product Research and Development* **1978**, 17 (1), 3-7.
56. Robeson, L. M., Miscible blends of poly(vinyl chloride) and poly(butylene terephthalate). *Journal of Polymer Science: Polymer Letters Edition* **1978**, 16 (6), 261-265.

57. Chandler, D., Interfaces and the driving force of hydrophobic assembly. *Nature* **2005**, 437 (7059), 640-647.
58. Gun'ko, V. M.; Mironyuk, I. F.; Zarko, V. I.; Turov, V. V.; Voronin, E. F.; Pakhlov, E. M.; Goncharuk, E. V.; Leboda, R.; Skubiszewska-Zięba, J.; Janusz, W.; Chibowski, S.; Levchuk, Y. N.; Klyueva, A. V., Fumed Silicas Possessing Different Morphology and Hydrophilicity. *Journal of Colloid and Interface Science* **2001**, 242 (1), 90-103.
59. Ran, C.; Ding, G.; Liu, W.; Deng, Y.; Hou, W., Wetting on Nanoporous Alumina Surface: Transition between Wenzel and Cassie States Controlled by Surface Structure. *Langmuir* **2008**, 24 (18), 9952-9955.
60. Cassie, A. B. D.; Baxter, S., Wettability of porous surfaces. *Transactions of the Faraday Society* **1944**, 40 (0), 546-551.
61. Xu, Q. F.; Wang, J. N.; Sanderson, K. D., Organic-Inorganic Composite Nanocoatings with Superhydrophobicity, Good Transparency, and Thermal Stability. *ACS Nano* **2010**, 4 (4), 2201-2209.
62. Yildirim, A.; Chattaraj, R.; Blum, N. T.; Goldscheitter, G. M.; Goodwin, A. P., Stable Encapsulation of Air in Mesoporous Silica Nanoparticles: Fluorocarbon-Free Nanoscale Ultrasound Contrast Agents. *Advanced healthcare materials* **2016**, 5 (11), 1290-1298.
63. Kaptay, G., On the equation of the maximum capillary pressure induced by solid particles to stabilize emulsions and foams and on the emulsion stability diagrams. *Colloids and Surfaces A: Physicochemical and Engineering Aspects* **2006**, 282-283, 387-401.
64. Prasad, V.; Semwogerere, D.; Eric, R. W., Confocal microscopy of colloids. *Journal of Physics: Condensed Matter* **2007**, 19 (11), 113102.
65. Kutuzov, S.; He, J.; Tangirala, R.; Emrick, T.; Russell, T. P.; Boker, A., On the kinetics of nanoparticle self-assembly at liquid/liquid interfaces. *Physical Chemistry Chemical Physics* **2007**, 9 (48), 6351-6358.
66. Steinberg, V.; Sütterlin, R.; Ivlev, A. V.; Morfill, G., Vertical Pairing of Identical Particles Suspended in the Plasma Sheath. *Physical Review Letters* **2001**, 86 (20), 4540-4543.
67. Davankov, V.; Tsyurupa, M.; Ilyin, M.; Pavlova, L., Hypercross-linked polystyrene and its potentials for liquid chromatography: a mini-review. *Journal of Chromatography A* **2002**, 965 (1), 65-73.
68. Berry, J. D.; Neeson, M. J.; Dagastine, R. R.; Chan, D. Y. C.; Tabor, R. F., Measurement of surface and interfacial tension using pendant drop tensiometry. *Journal of Colloid and Interface Science* **2015**, 454 (Supplement C), 226-237.
69. Vargaftik, N. B.; Volkov, B. N.; Voljak, L. D., International Tables of the Surface Tension of Water. *Journal of Physical and Chemical Reference Data* **1983**, 12 (3), 817-820.

70. Paunov, V. N., Novel Method for Determining the Three-Phase Contact Angle of Colloid Particles Adsorbed at Air–Water and Oil–Water Interfaces. *Langmuir* **2003**, *19* (19), 7970-7976.
71. Li, Z.; Giese, R. F.; van Oss, C. J.; Yvon, J.; Cases, J., The Surface Thermodynamic Properties of Talc Treated with Octadecylamine. *Journal of Colloid and Interface Science* **1993**, *156* (2), 279-284.
72. San-Miguel, A.; Behrens, S. H., Influence of Nanoscale Particle Roughness on the Stability of Pickering Emulsions. *Langmuir* **2012**, *28* (33), 12038-12043.
73. Korhonen, J. T.; Huhtamäki, T.; Ikkala, O.; Ras, R. H. A., Reliable Measurement of the Receding Contact Angle. *Langmuir* **2013**, *29* (12), 3858-3863.
74. Marmur, A., Soft contact: measurement and interpretation of contact angles. *Soft Matter* **2006**, *2* (1), 12-17.
75. Cwikel, D.; Zhao, Q.; Liu, C.; Su, X.; Marmur, A., Comparing Contact Angle Measurements and Surface Tension Assessments of Solid Surfaces. *Langmuir* **2010**, *26* (19), 15289-15294.
76. Decker, E. L.; Frank, B.; Suo, Y.; Garoff, S., Physics of contact angle measurement. *Colloids and Surfaces A: Physicochemical and Engineering Aspects* **1999**, *156* (1), 177-189.
77. Andrieu, C.; Sykes, C.; Brochard, F., Average Spreading Parameter on Heterogeneous Surfaces. *Langmuir* **1994**, *10* (7), 2077-2080.
78. Tsao, J. W. Influence of Nanoscale Roughness on Wetting Behavior in Liquid/Liquid Systems. Georgia Institute of Technology, Georgia Institute of Technology, 2014.
79. Murdock, R. C.; Braydich-Stolle, L.; Schrand, A. M.; Schlager, J. J.; Hussain, S. M., Characterization of Nanomaterial Dispersion in Solution Prior to In Vitro Exposure Using Dynamic Light Scattering Technique. *Toxicological Sciences* **2008**, *101* (2), 239-253.
80. Hassan, P. A.; Rana, S.; Verma, G., Making Sense of Brownian Motion: Colloid Characterization by Dynamic Light Scattering. *Langmuir* **2015**, *31* (1), 3-12.
81. Filipe, V.; Hawe, A.; Jiskoot, W., Critical Evaluation of Nanoparticle Tracking Analysis (NTA) by NanoSight for the Measurement of Nanoparticles and Protein Aggregates. *Pharmaceutical Research* **2010**, *27* (5), 796-810.
82. Francis, L. F.; Stadler, B. J. H.; Roberts, C. C., 2.2.3.2 Powder Fabrication. In *Materials Processing - A Unified Approach to Processing of Metals, Ceramics and Polymers*, Elsevier.
83. Zeppieri, S.; Rodríguez, J.; López de Ramos, A. L., Interfacial Tension of Alkane + Water Systems. *Journal of Chemical & Engineering Data* **2001**, *46* (5), 1086-1088.

84. Aranda-Bravo, C. G.; Romero-Martínez, A.; Trejo, A.; Águila-Hernández, J., Interfacial Tension and Density of Water + Branched Hydrocarbon Binary Systems in the Range 303–343 K. *Industrial & Engineering Chemistry Research* **2009**, *48* (3), 1476-1483.
85. Aveyard, R.; Haydon, D. A., Thermodynamic properties of aliphatic hydrocarbon/water interfaces. *Transactions of the Faraday Society* **1965**, *61* (0), 2255-2261.
86. Saien, J.; Akbari, S., Interfacial Tension of Toluene + Water + Sodium Dodecyl Sulfate from (20 to 50) °C and pH between 4 and 9. *Journal of Chemical & Engineering Data* **2006**, *51* (5), 1832-1835.
87. Kim, Y.; Wellum, G.; Mello, K.; Strawhecker, K. E.; Thoms, R.; Giaya, A.; Wyslouzil, B. E., Effects of relative humidity and particle and surface properties on particle resuspension rates. *Aerosol Science and Technology* **2016**, *50* (4), 339-352.
88. Birdi, K. S., *Scanning Probe Microscopes: Applications in Science and Technology*. CRC Press: 2003.
89. Zhao, J.; Jiang, S.; Wang, Q.; Liu, X.; Ji, X.; Jiang, B., Effects of molecular weight, solvent and substrate on the dewetting morphology of polystyrene films. *Applied Surface Science* **2004**, *236* (1), 131-140.
90. Lee, J.; Zhou, Z.-L.; Behrens, S. H., Characterizing the Acid/Base Behavior of Oil-Soluble Surfactants at the Interface of Nonpolar Solvents with a Polar Phase. *The Journal of Physical Chemistry B* **2015**, *119* (22), 6628-6637.
91. Van Oss, C. J.; Chaudhury, M. K.; Good, R. J., Interfacial Lifshitz-van der Waals and polar interactions in macroscopic systems. *Chemical Reviews* **1988**, *88* (6), 927-941.